A common molecular mechanism underlies the role of Mps1 in chromosome biorientation and the spindle assembly checkpoint

Giorgia Benzi, Alain Camasses, Yoshimura Atsunori, Yuki Katou, Katsuhiko Shirahige, Simonetta Piatti

A common molecular mechanism underlies the role of Mps1 in chromosome biorientation and the spindle assembly checkpoint

Giorgia Benzi, Alain Camasses[¶], Yoshimura Atsunori[§], Yuki Katou[§], Katsuhiko Shirahige[§] and Simonetta Piatti*

CRBM, University of Montpellier, CNRS

1919 Route de Mende

34293 Montpellier (France)

[¶]Institute of Molecular Genetics

1919 Route de Mende

34293 Montpellier (France)

[§]Institute of Molecular and Cellular Biosciences

The University of Tokyo

1-1-1 Yayoi, Bunkyo-ku,

Tokyo 113-0032 (Japan)

*Corresponding author: simonetta.piatti@crbm.cnrs.fr

Running title: Mps1 in chromosome biorientation

ABSTRACT

The conserved Mps1 kinase corrects improper kinetochore-microtubule attachments, thereby ensuring chromosome biorientation. Yet, its critical targets in this process remain elusive. Mps1 is also involved in the spindle assembly checkpoint (SAC), the surveillance mechanism halting chromosome segregation until biorientation is attained. Its role in SAC activation is antagonized by the PP1 phosphatase and involves phosphorylation of Knl1/Spc105, which recruits Bub1 to kinetochores to promote assembly of SAC effector complexes. A crucial question is whether error correction and SAC activation are part of a single device or separable pathways. Here we characterise a novel yeast mutant, *mps1-3*, defective in chromosome biorientation and SAC activation. Through an unbiased screen for suppressors, we found that mutations lowering PP1 levels at Spc105 or forced association of Bub1 with Spc105 reinstate both chromosome biorientation and SAC signalling in *mps1-3* cells. Our data strongly argue that Mps1-dependent phosphorylation of the Knl1/Spc105 kinetochore scaffold is critical for Mps1 function in both chromosome biorientation and SAC activation, thus supporting the idea that a common sensory apparatus simultaneously elicits error correction and SAC signalling.

INTRODUCTION

Accurate chromosome segregation is a fundamental aspect of mitosis and secures the genetic stability of a cell lineage. During the mitotic cell cycle, sister chromatids that have been generated by chromosome replication in S phase must attach through their kinetochores to microtubules emanating from opposite spindle poles in M phase. This occurs through an error correction mechanism where kinetochores dynamically attach and detach from microtubules until bipolar arrangement of sister chromatids is finalized (reviewed in Lampson and Grishchuk, 2017). Bipolar attachment, also referred to as amphitelic attachment, leads to tension across kinetochores, which arises from the balance of pulling forces exerted by microtubules and counteracting forces exerted by sister chromatid cohesion (reviewed in Bloom and Yeh, 2010). This tug of war leads also to chromosome congression to the metaphase plate.

Key to the error correction process is the evolutionary conserved CPC (chromosome passenger complex) that is composed by the Aurora B kinase and three additional centromere-targeting and activating subunits (INCENP, survivin and borealin). The CPC detects lack of kinetochore tension (e.g. in case of monotelic attachment where only one sister kinetochore is bound to microtubules or syntelic attachment where both sister kinetochores are attached to the same spindle pole) and favors amphitelic attachments by destabilizing incorrect kinetochore-microtubule connections through phosphorylation of specific kinetochore substrates (reviewed in Carmena et al., 2012). The Mps1 kinase is also required for the error correction pathway in many organisms (Jelluma et al., 2008; Jones et al., 2005; Maure et al., 2007; Santaguida et al., 2010; Storchová et al., 2011). In human cells Mps1 acts in concert with Aurora B in this process (Santaguida et al., 2010; Saurin et al., 2011; van der Waal et al., 2012). Additionally, Mps1-specific phosphorylation targets, like the kinetochore Ska complex, have been recently involved in the error correction mechanism (Maciejowski et al.,

2017). Importantly, in budding yeast Mps1 seems to operate independently of Aurora B in chromosome biorientation and its critical targets are unknown (Kalantzaki et al., 2015; Maure et al., 2007; Storchová et al., 2011). Although the budding yeast functional orthologue of the SKA complex, the Dam1 complex, is phosphorylated by Mps1, mutations altering these phosphorylations have no impact on chromosome segregation (Kalantzaki et al., 2015; Shimogawa et al., 2006).

The error correction process is intimately coupled to a conserved surveillance device, the Spindle Assembly Checkpoint or SAC, that prevents sister chromatid separation and the onset of anaphase until all chromosomes are bioriented on spindle microtubules. SAC signaling fires at unattached kinetochores, where SAC proteins are recruited, and is propagated to the whole cell for inhibition of the E3 ubiquitin ligase Anaphase Promoting Complex (APC) bound to its activator Cdc20. A soluble protein complex called MCC (Mitotic Checkpoint Complex) and composed of the SAC components Bub3, BubR1, Mad2 and Cdc20 is essential for APC/Cdc20 inhibition. This, in turn, prevents degradation of APC substrates, such as securin and cyclin B, thereby halting the cell cycle before the onset of anaphase (reviewed in Musacchio, 2015).

The Mps1 kinase acts at the apex of the SAC signaling pathway, by phosphorylating the Knl1/Spc105 kinetochore scaffold on its MELT repeats, which in turn recruit the Bub3-Bub1 SAC complex (London et al., 2012; Primorac et al., 2013; Shepperd et al., 2012; Yamagishi et al., 2012). Subsequent binding of the SAC factor Mad1 to Bub1, together with Mps1-mediated Mad1 phosphorylation, is a prerequisite for recruitment of Mad2 to kinetochores and MCC assembly (Ji et al., 2017; London and Biggins, 2014; Mora-Santos et al., 2016; Moyle et al., 2014; Zhang et al., 2017). Consistently, phosphorylation of Knl1/Spc105 MELT repeats by Mps1 is essential for SAC signaling (London et al., 2012; Shepperd et al., 2012; Yamagishi et al., 2012). The Knl1/Spc105 kinetochore protein has emerged as a key factor

not only as a platform for SAC signaling, but also to silence the SAC once all pairs of sister chromatids are bipolarly attached. Indeed, Knl1/Spc105 harbors at its N-terminus an "RVSF" aminoacid motif that binds to PP1, which extinguishes SAC silencing at least partly by dephosphorylating Knl1/Spc105 MELT repeats (Bokros et al., 2016; Liu et al., 2010; Meadows et al., 2011; Pinsky et al., 2009; Rosenberg et al., 2011; Vanoosthuyse and Hardwick, 2009). Additionally, PP1 dephosphorylates the catalytic loop of Mps1, thus further silencing SAC (Moura et al., 2017).

Aurora B has also been implicated in SAC signaling. While an early model proposed that its role in the SAC would be indirect and linked to the generation of unattached kinetochores during the correction of tension-less kinetochore-microtubule attachments (Ditchfield et al., 2003; Hauf et al., 2003; King et al., 2007; Pinsky et al., 2006), increasing evidence supports a direct role of Aurora B in SAC activation from unattached kinetochores (Kallio et al., 2002; Maldonado and Kapoor, 2011; Petersen and Hagan, 2003; Santaguida et al., 2011; Saurin et al., 2011; Vader et al., 2007). For instance, Aurora B promotes kinetochore recruitment of several SAC factors, including Mps1 and weakens PP1 binding to Knl1 through phosphorylation of Knl1 RVSF motif, suggesting that it acts upstream of SAC signaling (Ditchfield et al., 2003; Hewitt et al., 2010; Liu et al., 2010; Santaguida et al., 2010; Saurin et al., 2011).

The involvement of Mps1 and Aurora B in both error correction and SAC signaling raises a crucial, yet unsolved, question: are these two pathways concomitantly elicited by a common upstream sensory device or, alternatively, they respond to distinct defects (i.e. lack of kinetochore tension and lack of kinetochore attachment)? Is it possible to activate SAC without engaging the error correction machinery and vice versa? If the molecular machineries

detecting these defects were separable, it should be possible to generate hypo- or hyper-morphic mutants in the two apical kinases that selectively affect either pathway without perturbing the other.

Here we report the characterization of a novel temperature-sensitive *mps1* mutant of budding yeast (named *mps1-3*) that is defective in chromosome biorientation and SAC signaling. An unbiased genetic screen for extragenic suppressors of the lethality of *mps1-3* cells at high temperature revealed that mutations affecting the Spc105-PP1 interface restore proper chromosome biorientation as well as a proficient SAC response. Furthermore, artificial anchoring of Bub1 near the MELT repeats of Spc105 in *mps1-3* cells results in a similar rescue. Altogether, our data indicate that Mps1 promotes both error correction and SAC signaling through a common molecular mechanism based on Spc105 phosphorylation at the MELT repeats and recruitment of the Bub1 kinase to kinetochores, thereby strengthening the idea that a single sensory apparatus engages both processes.

RESULTS

The novel *mps1-3* mutant is defective in chromosome segregation and proficient in SPB duplication

The targets of budding yeast Mps1 in the error correction pathway are unknown so far. Dissecting the function of Mps1 in kinetochore error correction is hampered by its involvement in the duplication of spindle pole bodies (SPBs) and the assembly of a bipolar spindle (Weiss and Winey, 1996), the first step towards chromosome biorientation.

We isolated the *mps1-3* mutant through a random mutagenesis screen for temperature-sensitive *mps1* mutants (see Materials and Methods). Haploid *mps1-3* cells grew slowly at 25°C-30°C and were unable to form colonies at temperatures above 32°C (Fig. 1A). Sequencing of the *mps1-3* allele revealed a single mutation replacing the conserved serine 635 in the kinase domain by phenylalanine (Fig. 1B). To characterise the primary defects underlying the temperature-sensitivity of *mps1-3* cells, we synchronised in G1 *mps1-3* cells, together with a wild type control and the well-characterised *mps1-1* mutant (Weiss and Winey, 1996), and released cells at the restrictive temperature of 34°C. FACS analysis of DNA contents revealed the expected bimodal distribution of DNA contents in wild type cells, while *mps1-3* and *mps1-1* cells showed a broad distribution of DNA contents after cytokinesis (90-105 minutes), indicative of massive chromosome missegregation (Fig. 1C). However, while *mps1-1* cells were unable to assemble bipolar spindles due to their failure to duplicate SPBs and to activate the SAC (Weiss and Winey, 1996), *mps1-3* cells proficiently formed bipolar spindles and elongated them during anaphase (Fig. 1D and S1A), suggesting that *mps1-3* might be a separation of function mutant specifically defective in chromosome biorientation but proficient at SPB duplication.

To quantify the *mps1-3* chromosome segregation defects we used a genetic assay based on the ability of diploid cells to mate with a haploid tester strain upon events leading to loss of one of the two copies of the *MAT* locus, including loss of one entire chromosome III (Andersen et al., 2008). We used wild type and homozygous *mps1-1*/*mps1-1*, *mps1-3*/*mps1-3* diploid cells that were grown for a defined number of generations at 25°C. Already under these permissive conditions the appearance of mating-competent cells was 1000-2000 fold higher in the *mps1* mutants relative to the wild type (Fig. 1E), suggesting pronounced chromosome loss even in conditions that allow cell proliferation.

To follow directly chromosome biorientation in *mps1-3* haploid cells, we visualized by fluorescence microscopy the segregation of chromosome V tagged with the TetO/TetR system 1.4kb from the centromere (*CEN5-GFP*) (Tanaka et al., 2000). Cells were also expressing the SPB marker Spc97-mCherry and carried a *cdc15-2* temperature-sensitive allele to arrest cells in telophase. G1-synchronised cells were released at the restrictive temperature of 34°C and samples were collected at 120 and 150 minutes from the release. As expected, near the totality of wild type cells bioriented and properly segregated the two sister chromatids of chromosome V at opposite SPBs, while almost all *mps1-1* cells underwent *CEN5* mono-orientation on the single unduplicated SPB (Fig. 1F). Strikingly, the vast majority of the *mps1-3* mutant cells displayed duplicated SPBs that separated far apart, but at 120' the two chromatids had segregated correctly to opposite spindle poles in 42% of the cells, whereas in 41% of the cells the two chromatids had remained at the same spindle pole. Only 4% of the cells did not duplicate the SPBs, while 12% of the cells had duplicated SPBs that remained very close to each other in the mother cell, accompanied by lack of *CEN5* segregation (Fig. 1F). We conclude that the *mps1-3* mutant, although capable to duplicate the SPBs and form bipolar spindles, is specifically defective in chromosome biorientation at 34°C. It is worth

noting, however, that at higher temperatures (37°C) *mps1-3* cells also failed SPB duplication and bipolar spindle assembly, suggesting that *mps1-3* is a hypomorphic mutant.

Centromeric and pericentromeric cohesin is crucial for chromosome biorientation, but while centromeres transiently split in metaphase upon bipolar attachment, pericentromeric cohesion resists to pulling spindle forces (Tanaka et al., 2000). We therefore asked if premature loss of pericentromeric cohesion could underlie the chromosome biorientation defect of *mps1-3* cells. To answer this question, we tagged with the TetO/TetR system the pericentromere of chromosome V (TetO array at -13kb from the centromere, (Tanaka et al., 2000)) and analysed its behaviour in metaphase-arrested cells by fluorescence microscopy. After a pre-synchronisation in G1, cells carrying the temperature-sensitive *cdc16-1* allele (compromising APC/C activity at high temperatures and arresting cells in metaphase (Irniger et al., 1995)) were released at 34°C. Under these conditions, sister pericentromeric regions of chromosome V did not disjoin in most *mps1-3* cells, similar to wild type and *mps1-1* cells (Fig. S1B). Thus, the chromosome biorientation defect of *mps1-3* cells is not explained by a premature loss of pericentric cohesion.

Biorientation defects could be due to lack of kinetochore-microtubule attachments, or to a failure in the correction of faulty kinetochore-microtubule connections that are not under tension. To discriminate between these two processes, we imaged live cells with GFP-tagged *CEN5* and expressing Tub1-mCherry to visualize microtubules. Cells were pre-incubated at 34°C for 1 hour before filming at the same temperature. Under these conditions, while 100% of wild type cells correctly bioriented the two sister *CEN5* and segregated them to opposite spindle poles (n=201, Fig. 1G and 3H), only 51,3% of *mps1-3* mutant cells bioriented *CEN5*, whereas 48,7% of the cells did not (n=179, Fig. 1G and 3H). During the whole movie we did not detect lagging chromosomes or *CEN5* signals off the spindle in *mps1-3* cells, suggesting that kinetochore-microtubule attachment is not affected. Furthermore, in contrast to *ipl1*

mutant cells that missegregate chromosomes mostly towards the old SPB (Tanaka et al., 2002), we found no such bias in *mps1-3* cells under the above conditions (Fig. 3H). Interestingly, however, when we filmed *mps1-3* after a G1 arrest and release at 34°C (i.e. during the first cell cycle at restrictive temperature, when the pre-existing SPB is likely fully functional) we found a strong missegregation bias towards the bud (Fig. S1C). This bias tends to be lost in the subsequent cell cycles (Fig. S1C). From these data we conclude that *mps1-3* cells are defective in the correction of monopolar attachments, like *ipl1* mutants and in agreement with previous conclusions (Maure et al., 2007). Additionally, they could alter the normal pattern of SPB asymmetric inheritance (see Discussion).

The *mps1-3* mutant does not engage the spindle assembly checkpoint

To assess if *mps1-3* cells can engage the SAC, pre-synchronised G1 cells were released at 34°C in presence of the microtubule-depolymerizing drug nocodazole. FACS analysis of DNA contents showed that wild type cells arrested as expected in metaphase with 2C DNA contents, indicative of proficient SAC signalling. Contrariwise, *mps1-3* and *mps1-1* cells kept progressing through the cell cycle accumulating 4C DNA contents, indicating that they cannot engage a SAC response (Fig. 2A). This was confirmed by western blot analysis of two APC substrates, the securin Pds1 and the cyclin B Clb2, which are normally degraded in anaphase and stabilised by the SAC. As expected, both proteins remained stable in wild type cells treated with nocodazole, while they underwent proteolysis in *mps1-1* and *mps1-3* mutants (Fig. 2B). Thus, the *mps1-3* mutant is severely defective in SAC activation at high temperature.

The Mps1-3 mutant protein has enhanced kinase activity but has reduced levels at kinetochores

The catalytic activity of Mps1 is essential for both chromosome biorientation and SAC activation (Jones et al., 2005; London et al., 2012; Maure et al., 2007; Storchová et al., 2011). In order to understand if the defects of the *mps1-3* mutant were due to impaired Mps1 kinase activity, we performed *in vitro* kinase assays using recombinant Mps1 and Mps1-3 proteins purified from bacteria. We measured the ability of these proteins to auto-phosphorylate and to phosphorylate the N-terminal part of Spc105 (aa 1-320) at different times of incubation in the presence of $P^{33}\gamma$ATP at 34°C. Surprisingly, the Mps1-3 catalytic activity turned out to be more elevated than that of Mps1 at all-time points (Fig. 2C). This was confirmed by similar kinase assays in the presence of the exogenous substrate MBP and Mps1/Mps1-3 proteins affinity-purified from yeast cells using galactose-inducible glutathione *S*-transferase (GST) fusion constructs (Lauzé et al., 1995) (Fig. S2A). Contextually, Mps1-3 protein levels in yeast cells were also 2-3 fold higher than wild type Mps1 and had aberrant electrophoretic mobility (Fig. S2A). The elevated Mps1-3 levels correlated with a decreased proteolysis of the protein in mitosis (Fig. S2B), consistent with the idea that Mps1 turnover inversely correlates to its kinase activity (Palframan et al., 2006).

Since Mps1 levels at kinetochores increase when its kinase activity is inactivated (Hayward et al., 2019; Hewitt et al., 2010; Jelluma et al., 2010; Santaguida et al., 2010; Wang et al., 2014), it is conceivable that the elevated Mps1 kinase activity in *mps1-3* cells accelerates Mps1 kinetochore turnover to a threshold that could be incompatible with SAC signalling and chromosome biorientation. To test this possibility, we tagged with three HA epitopes the *MPS1* and *mps1-3* genes at their genomic locus and checked the distribution of the corresponding proteins on chromosomes by ChIP-seq using cells pre-synchronised in G1 and released in nocodazole for 90 minutes at 34°C, time at which both *MPS1* and *mps1-3* cells were still in mitosis. Strikingly, while wild type Mps1 clearly accumulated at the centromeric

region of all 16 yeast chromosomes, Mps1-3 did not (Fig. 2D and S3), suggesting that its residence at kinetochores is severely impaired.

To definitely ascertain if reduced kinetochore levels are the main reason for the Mps1-3 loss of function, we artificially recruited to kinetochores GFP-tagged Mps1 and Mps1-3 in cells that co-expressed the kinetochore protein Mtw1 tagged with the high affinity GFP-nanotrap (GFP-binding domain or GBD) (Rothbauer et al., 2008). This strategy led to constitutive association of Mps1 to the kinetochore in 91,3% of the cells and of Mps1-3 in 88,5% of the cells (n=196 and n=209, respectively). Cells also carried the deletion of *MAD2* to obliterate SAC, which would be otherwise constitutively active following Mps1 tethering to kinetochores (Aravamudhan et al., 2015; Jelluma et al., 2010). Notably, anchoring Mps1-3 to Mtw1 could partially restore proper chromosome segregation at 34°C, as shown by the bimodal distribution of DNA contents by FACS analysis (Fig. 2E), suggesting that the chromosome biorientation defects of *mps1-3* cells are largely accounted for by decreased Mps1 kinetochore levels.

A genetic screen for spontaneous suppressors of the *mps1-3* mutation

Since SAC is not essential in budding yeast (Hoyt et al., 1991; Li and Murray, 1991), we reasoned that chromosome missegregation could be the main cause of the lethality of *mps1-3* cells at high temperatures, which makes this mutant a unique genetic tool to study the role of Mps1 in chromosome biorientation. To gain insights into this process, we performed an unbiased genetic screen for spontaneous mutations suppressing the temperature-sensitivity of *mps1-3* cells at 34°C. Classical genetic analyses allowed us to establish if the suppressing mutations were recessive or dominant, distinguish the intragenic from the extragenic suppressors (i.e. suppressing mutation inside or outside the *mps1-3* gene, respectively) and assess if the extragenic suppressors were allelic to one another. Through this screen we could

isolate 27 suppressors. Out of these, 17 turned out to be intragenic while 10 were extragenic suppressors. We focused on the extragenic suppressors, which could provide valuable insights into the molecular mechanism underlying the role of Mps1 in chromosome biorientation. Through genetic analyses and whole genome sequencing, we could establish that the suppressing mutations hit three different genes (Fig. 3A, B): *SPC105*, encoding for the kinetochore protein Spc105/Knl1; *GLC7*, encoding for the catalytic subunit of the phosphatase PP1; *GRR1*, encoding for an F-box protein of the E3 ubiquitin ligase complex SCF. Three *GRR1* suppressors out of four carried also a mutation in *RSC30*, encoding for a subunit of the RSC chromatin-remodelling complex (Angus-Hill et al., 2001). The basis for the suppression by the *GRR1* mutations, alone or in combination with the mutation in *RSC30*, was not immediately clear and will be investigated in the future.

Spc105 (Knl1 in metazoans) is a known target of Mps1 in the SAC (London et al., 2012). Mps1-dependent phosphorylation of its MELT repeats is crucial for SAC signalling by recruiting Bub1 and Bub3 (London et al., 2012; Primorac et al., 2013; Shepperd et al., 2012; Yamagishi et al., 2012). The PP1 Glc7 in turn dephosphorylates Spc105 MELT repeats by binding directly the consensus RV/IXF motif at the N-terminus of Spc105 (RVSF, aa 75-78) to release Bub1 and silence the checkpoint (London et al., 2012; Rosenberg et al., 2011). Strikingly, all our suppressing mutations in *SPC105* encompassed or were close to the PP1-binding motif, while both *GLC7* suppressors carried a missense mutation of Phe256 (to Ile or Val), which resides in the hydrophobic groove involved in PP1 interaction with partners carrying the RV/IXF consensus motif (Wu and Tatchell, 2001) (Fig. 3B). Collectively, these observations suggest that reduced PP1 interaction with Spc105 likely accounts for the rescue of the temperature-sensitivity of *mps1-3* cells. Interestingly, the *spc105-V76G* mutation was recessive and lethal in otherwise wild type cells, consistent with the notion that mutations in the PP1-binding site of Spc105 are inviable due to constitutive SAC activation (Rosenberg et

al., 2011), while *spc105-A79T* and *spc105-V82D* were viable, suggesting that they might interfere with PP1 recruitment to kinetochores less severely than *spc105-V76G*. It is also worth noting that *spc105-V76G* suppressed more robustly than *spc105-A79T* and *spc105-V82D* the lethality of *mps1-3* cells at high temperatures (Fig. 3A).

Consistent with the idea that lack of PP1 recruitment to Spc105 rescues the lethality of *mps1-3* cells, the well characterized *RASA* mutation in the PP1 binding motif of Spc105 (Rosenberg et al., 2011) also suppressed the temperature-sensitivity of *mps1-3* cells (Fig. 3C; note that the *spc105-RASA* mutation is lethal unless SAC activity is abolished, e.g. by *MAD2* deletion (Rosenberg et al., 2011)). Additionally, fusing the PP1 catalytic subunit Glc7 to the N-terminus of the Spc105-RASA mutant protein (Rosenberg et al., 2011) almost completely abolished its suppressing properties (Fig. 3C), indicating that suppression stems only from loss of PP1 binding to Spc105.

The *GLC7* mutations isolated in our screen were dominant and viable in otherwise wild type cells. Since dominant mutations are often associated with gain of function, this observation was quite puzzling and prompted us to characterise PP1 activity in *GLC7-24* cells. As a readout, we analysed the phosphorylation status of the well-characterised PP1 cytoplasmic substrate Snf1, which is hyperphosphorylated on T210 under low glucose conditions (1%) and gets dephosphorylated by Glc7 in high glucose (4%) (Rubenstein et al., 2008). No significant differences in the phosphorylation of Snf1 T210 were apparent in *mps1-3 GLC7-24* and *GLC7-24* cells relative to the wild type (Fig. S4A), suggesting that the cytoplasmic activity of PP1 is not affected. To assess PP1 phosphatase activity at kinetochores in *GLC7-24* cells, we monitored phosphorylation of Sli15, a subunit of the Aurora B complex that resides at kinetochores and on spindle microtubules and is involved in chromosome biorientation (Kim et al., 1999; Tanaka et al., 2002). Sli15 is phosphorylated by Ipl1/Aurora B (Nakajima et al., 2011), whose activity is often reversed by PP1 (Francisco et al., 1994; Hsu et al., 2000).

Interestingly, Sli15 phosphorylation was more pronounced in cycling cells and slightly advanced during the cell cycle in the *GLC7-24* mutant relative to the wild type (Fig. S4B). Thus, Glc7 phosphatase activity is not globally elevated in *GLC7-24* cells; rather, it might impair dephosphorylation of specific kinetochore substrates.

Suppressing mutations in *SPC105* and *GLC7* restore SAC activation and normal chromosome segregation in *mps1-3* cells

To investigate further the phenotypes of the suppressors, we analysed their ability to engage the SAC and undergo normal chromosome segregation. Pre-synchronised G1 cells were released at 34°C in the presence and absence of nocodazole and subjected to FACS analysis of DNA contents at different time points. Importantly, the *spc105-18* and *GLC7-24* mutations restored proficient SAC activation in *mps1-3* cells (Fig. 3D). In *mps1-3 GLC7-24* cells this was accompanied by Mad1 hyperphosphorylation, which requires Mps1 activity (Hardwick et al., 1996; Hardwick and Murray, 1995) and was abolished in *mps1-3* cells (Fig. 3E; note that we could not study Mad1 phosphorylation pattern in *mps1-3 spc105-18* cells due to their synthetic lethality with HA-tagged Mad1). Since Mad1 is recruited to unattached kinetochores and is not part of soluble MCC (Fraschini et al., 2001b; Gillett et al., 2004), these data further strengthen the idea that in *GLC7-24* cells PP1 has impaired ability to dephosphorylate kinetochore substrates. Additionally, they raise the possibility that PP1 could dephosphorylate Mad1 directly.

Remarkably, the *spc105-18* and *GLC7-24* suppressors also rescued the chromosome segregation defects of *mps1-3*, as shown by the bimodal distribution of DNA contents after one complete cell cycle at 34°C (Fig. 3F). Moreover, live cell imaging of *mps1-3 spc105-18* and *mps1-3 GLC7-24* cells with GFP-tagged *CEN5* and expressing Tub1-mCherry showed nearly complete suppression of chromosome missegregation (Fig. 3G-H). Importantly, the

spc105-18 and *GLC7-24* alleles did not restore normal levels of Mps1-3 at centromeres, as shown by ChIP-seq (Fig. 3I and S5). Furthermore, suppression of chromosome missegregation was not a consequence of restored SAC activity, which might impose sufficient time for error correction, because it remained unchanged upon *MAD2* deletion (Fig. 3H).

Thus, these data strongly argue that a common mechanism involving Mps1 and antagonized by PP1 simultaneously promotes error correction of faulty kinetochore attachments and SAC signalling.

The *spc105-18* and *GLC7-24* suppressors restore Spc105 phosphorylation in *mps1-3* cells

To further explore the possibility that Mps1 could promote SAC signalling and chromosome biorientation through the same molecular mechanism, we analysed the phosphorylation status of Spc105 in wild type and *mps1-3* cells at 34°C in presence or absence of nocodazole. As expected, Spc105 tagged with 3HA (Spc105-3HA) was promptly phosphorylated in wild type cells treated with nocodazole, as indicated by its mobility shift in SDS page (times 60-150 minutes after release from G1, Fig. 4A). Phosphorylation was impaired in *mps1-3* cells under the same conditions, in agreement with the notion that Spc105 is a critical Mps1 substrate during SAC activation (London et al., 2012). Importantly, Spc105 phosphorylation was efficiently restored, if not accentuated, in the *mps1-3 spc105-18* and *mps1-3 GLC7-24* mutants (Fig. 4A), consistent with defective PP1 activity at kinetochores that counteracts Mps1-dependent phosphorylation of Spc105 during SAC signalling. Interestingly, we could detect a slight electrophoretic mobility shift of Spc105 also in wild type cells undergoing a normal cell cycle in the absence of nocodazole (Fig. 4B, times 30'-40' after release from G1, which corresponds to cells in S phase), suggesting that Mps1 might phosphorylate a low number of MELT repeats in unperturbed conditions. Consistent with this hypothesis, an

unphosphorylatable MELT mutant (*spc105-6A*) is unable to recruit Bub1 to kinetochores also during unperturbed conditions and displays chromosome segregation defects (London et al., 2012). Spc105 phosphorylation was not apparent in *mps1-3* cells at 34°C and was restored in *mps1-3 spc105-18* cells (Fig. 4B). It is worth noting that the mobility shift of Spc105 was even more conspicuous and present for a larger cell cycle window in *mps1-3 spc105-18* cells than in the wild type (Fig. 4B), in line with the impaired PP1 activity at Spc105 in this mutant. Moreover, it was prominent in *mps1-3 spc105-24* cells at 25°C, but less so at 34°C (Fig. S6A), confirming that it depends on Mps1 activity at kinetochores.

Bub1 recruitment to kinetochores is impaired in *mps1-3* cells but is restored by the *spc105-18* and *GLC7-24* suppressing mutations

As mentioned above, Spc105/Knl1 phosphorylation primes Bub1 recruitment to kinetochores for SAC signalling (London et al., 2012; Primorac et al., 2013; Shepperd et al., 2012; Yamagishi et al., 2012). Since Bub1 transiently associates with kinetochores also under unperturbed conditions (Gillett et al., 2004), we visualized by time-lapse video microscopy Bub1-GFP along with the kinetochore marker Mtw1-Tomato in wild type and *mps1-3* cells at 34°C. Under these conditions, Bub1 was transiently recruited to kinetochores in wild type cells with a small and medium bud, i.e. during S phase and early mitosis, in 100% of the cells (n=260, Fig. 4C, D). In *mps1-3* cells we detected low levels of Bub1 at kinetochores only in 20% of the cells at 34°C (n=170, Fig. 4C, D), while the protein co-localized normally with Mtw1 in small and medium budded cells at 25°C (Fig. S6B). Therefore, lack of Spc105 phosphorylation in *mps1-3* cells under unperturbed conditions correlates with loss of Bub1 at kinetochores. Remarkably, Bub1 kinetochore localisation was restored to nearly wild type levels in *mps1-3 spc105-18* and *mps1-3 GLC7-24* cells (Fig. 4C, D), further strengthening the correlation between Spc105 phosphorylation and Bub1 residence at kinetochores. It is worth

noting that while in wild type cells Bub1 dissociated from the kinetochores at the time of chromosome biorientation, it persisted at kinetochores up to anaphase in the majority of *mps1-3 spc105-18*, in good agreement with Spc105 hyperphosphorylation in these cells.

In order to be fully functional for SAC activation, Bub1 also needs to be directly phosphorylated by Mps1, which in turn allows its binding to Mad1 (Ji et al., 2017; London and Biggins, 2014; Mora-Santos et al., 2016). Thus, we checked if Bub1 phosphorylation was also impaired in *mps1-3* cells. Pre-synchronised G1 cells were released at 34°C in the presence or the absence of nocodazole. Although several forms of Bub1 with different electrophoretic mobility were present throughout the cell cycle, one particular isoform with slowest mobility appeared in the wild type at 20'after G1 release, i.e. when cells entered S phase, thus correlating with the timing of Bub1 kinetochore localization (Fig. 4E-H). While this hyper-phosphorylation was transient in the absence of nocodazole, disappearing by 60' (Fig. 4G), it accumulated upon microtubule depolymerisation in wild type cells (Fig. 4E). Under both conditions this isoform was not apparent in *mps1-3* cells, suggesting that it is phosphorylated by kinetochore-bound Mps1 (Fig. 4E, G). Furthermore, Bub1 hyper-phosphorylation was not restored in the *mps1-3 spc105-18* and *mps1-3 GLC7-24* suppressors undergoing cell cycle progression in the absence (Fig. S6C) or in the presence of nocodazole (Fig. S6D), although a modest Bub1 hyper-phosphorylation could be observed in the *mps1-3 GLC7-24* suppressor treated with nocodazole at late time points (Fig. S6D). Thus, the mechanism underlying the suppression of *mps1-3* mutant cells might be independent of the phosphorylation status of Bub1.

Since Bub1 has been involved in kinetochore biorientation in budding yeast (Fernius and Hardwick, 2007; Storchová et al., 2011), we conclude that lack of Bub1 recruitment to kinetochores is likely the main reason underlying the chromosome segregation defects of

mps1-3 cells. Lowering PP1 levels at Spc105 in the suppressors favours phosphorylation of the MELT repeats of Spc105, thereby restoring Bub1 recruitment at kinetochores and chromosome biorientation.

Artificial targeting of Bub1 to Spc105 restores proper chromosome segregation and SAC response in *mps1-3* cells

If our above conclusions are correct, artificial tethering of Bub1 to kinetochores could rescue the chromosome segregation defects of *mps1-3* cells at high temperatures. To test this hypothesis, we generated yeast strains expressing as sole source of Spc105 an Spc105 variant where we had inserted the GFP-binding domain upstream of the MELT repeats of Spc105 (Spc105-GBD). In the same strains we co-expressed Bub1-GFP or Bub3-GFP (note that although Bub3 enhances Bub1 binding to Spc105 by directly reading its phosphorylated MELT repeats, it has no additional role in Bub1 activation (Breit et al., 2015; Primorac et al., 2013)). This strategy led to constitutive recruitment of Bub1 to kinetochores throughout the cell cycle (Fig. 5A and movie S1), with no obvious impact on the proliferation rate of otherwise wild type cells (Fig. 5B), indicating that prolonged Bub1 residence at kinetochores is insufficient to constitutively activate the SAC. Artificial recruitment of Bub1 to Spc105 only modestly, if at all, rescued the lethality of *mps1-3* cells at high temperatures (Fig. 5B). However, it did prolong the viability of *mps1-3* cells after transient incubation at restrictive temperature (Fig. 5C), suggesting that proper chromosome segregation might be partially restored. In agreement with this hypothesis, FACS analysis of DNA contents in synchronised *mps1-3* cells, either lacking or carrying the *SPC105-GBD* and *BUB1-GFP* or *BUB3-GFP* constructs, showed that the massive chromosome missegregation of *mps1-3* cells at 34°C was partially (*BUB3-GFP*) or largely (*BUB1-GFP*) rescued, as indicated by the bimodal distribution of DNA contents (Fig. S7A and 5D). Interestingly, artificial anchoring of Bub1 to

Spc105 also partially suppressed the SAC defects of *mps1-3* cells (Fig. S7B). Nevertheless, the rescue of chromosome missegregation was independent of restored SAC signalling, as it remained unaffected by *MAD2* deletion (Fig. 5C, D). Thus, the main reason underlying the chromosome biorientation, and possibly SAC defects, of *mps1-3* cells is the lack of Bub1 at kinetochores.

The function of Mps1 and Bub1 in chromosome biorientation has been previously linked to pericentromeric localisation of Shugoshin, which in yeast requires Mps1 and Bub1 kinase activity (Fernius and Hardwick, 2007; Nerusheva et al., 2014; Peplowska et al., 2014; van der Waal et al., 2012). Shugoshin senses the lack of kinetochore tension and engages the error correction machinery through kinetochore recruitment of the CPC complex (chromosome passenger complex) (Indjeian et al., 2005; Kawashima et al., 2007; Nerusheva et al., 2014; Peplowska et al., 2014; Rivera et al., 2012; Vanoosthuyse et al., 2007; Verzijlbergen et al., 2014). Although the role of budding yeast Mps1 in chromosome biorientation seems independent of the CPC and Aurora B activity (Maure et al., 2007; Storchová et al., 2011), we decided to investigate if the chromosome segregation defects of *mps1-3* cells could be ascribed to poor Shugoshin activity at pericentromeres. Although co-localisation of Sgo1 (the only budding Shugoshin) with kinetochore clusters was partially compromised in *mps1-3* cells at 34°C (Fig. S8A), in agreement with previous observations (Storchová et al., 2011) and with the loss of Bub1 at kinetochores, *mps1-3* cells turned out to be synthetically lethal with *SGO1* deletion even at 25°C (Fig. S8B), strongly arguing against a linear pathway where Mps1 acts upstream of Sgo1.

The role of budding yeast Aurora B (Ipl1) in chromosome biorientation relies on its alternative targeting to centromeres or the inner kinetochore (Fischboeck et al., 2018; García-Rodríguez et al., 2019; Makrantoni and Stark, 2009). While centromeric localisation depends

on histone H2A phosphorylation by Bub1 and subsequent recruitment of Shugoshin and the Bir1 subunit of CPC (survivin in metazoans)(Kawashima et al., 2010, 2007), kinetochore localisation requires binding of Aurora B and the Sli15 subunit of CPC (INCENP in metazoans) to the COMA complex (Fischer et al., 2004; García-Rodríguez et al., 2019). A truncated Sli15 lacking its N-terminal region (Sli15-ΔNterm) or alanine mutations in its CDK-dependent phosphorylation sites (Sli15-6A) might favour Ipl1 binding to the COMA complex and/or microtubules (Fischböck-Halwachs et al., 2019; García-Rodríguez et al., 2019; Pereira and Schiebel, 2003) and, concomitantly, rescue the lethality/growth defects of *bir1Δ*, *bub1Δ* and *sgo1Δ* cells (Campbell and Desai, 2013). If the chromosome segregation defects of *mps1-3* cells arose exclusively from poor activity of centromeric Sgo1/CPC, then they should be similarly suppressed by the Sli15-ΔNterm and Sli15-6A variants. This was definitely not the case, as shown by proliferation assays (Fig. S8C) and FACS analysis of DNA contents on synchronised cells (Fig. S8D).

Finally, since Dam1 is a critical phosphorylation target of Ipl1 in the error correction process (Cheeseman et al., 2002; Kalantzaki et al., 2015), we monitored its phosphorylation state in wild type, *mps1-3* and *ipl1-321* cells during a synchronous release from G1 at 34°C. While the electrophoretic mobility of Dam1-3PK was dramatically altered by the *ipl1-321* mutation, it was mainly unaffected in *mps1-3* cells (Fig. S8E), consistent with the notion that phosphorylation of Dam1 by Mps1 is dispensable for chromosome biorientation (Kalantzaki et al., 2015; Shimogawa et al., 2006) and suggesting that Ipl1 kinase activity is largely proficient in *mps1-3* cells.

We therefore conclude that lack of Bub1 at kinetochores is mainly responsible for the chromosome biorientation flaws of *mps1-3* mutant cells, at least partly independently of the role of Bub1 in Sgo1 kinetochore recruitment and CPC activation.

DISCUSSION

The *mps1-3* mutant as a novel genetic tool to study the role of Mps1 in chromosome segregation

The precise function of budding yeast Mps1 in chromosome biorientation has been elusive so far. We have shed light on this process through the characterisation of the conditional *mps1-3* mutant that at 34°C is defective in this process but proficient at SPB duplication and bipolar spindle assembly. Our analysis of the segregation pattern of chromosome V in *mps1-3* cells suggests that each pair of sister chromatids has equal chance to segregate in a bipolar or monopolar fashion. This random segregation applied to the 16 yeast chromosomes makes the likelihood for each single *mps1-3* cell to segregate correctly all chromosomes extremely low (1.5×10^{-5}), which is in agreement with the massive chromosome missegregation we observe. Being *mps1-3* cells also SAC-deficient makes monopolar attachments undetected by the checkpoint, thus generating highly aneuploid cells.

We could establish through live cell imaging that *mps1-3* cells are not defective in kinetochore-microtubule attachment, but rather in the error correction mechanism that converts monotelic or syntelic linkages into amphitelic attachments, in agreement with previous conclusions (Maure et al., 2007; Storchová et al., 2011). This function has been classically attributed to Aurora B and the CPC (reviewed in Krenn and Musacchio, 2015), but in more recent years Mps1 has also been implicated in this process. Mps1 was shown to impact on Aurora B activity through phosphorylation of the CPC subunit borealin (Jelluma et al., 2008), as well as to act downstream of Aurora B (Santaguida et al., 2010), suggesting a complex interplay between the two kinases. In contrast, in budding yeast Mps1 and Aurora B (Ipl1) were proposed to operate independently (Maure et al., 2007; Storchová et al., 2011).

While *ipl1* mutants missegregate chromosomes preferentially towards the old SPB, presumably because the new SPB must undergo a maturation time before becoming fully able to nucleate microtubules (Tanaka et al., 2002), we find different results in *mps1-3* cells depending on the experimental conditions. In particular, during the first cell cycle at restrictive temperature *mps1-3* cells missegregate chromosomes preferentially towards the bud (i.e. towards the old SPB) similar to *ipl1* mutant cells. In contrast, during the following cell cycles this bias seems to be progressively lost. These results can be rationalised by surmising that Mps1 and Ipl1 are both involved in error correction of kinetochore attachments, but Mps1 could be additionally required for SPB maturation. In other words, when Mps1 activity is disabled, young SPBs fail to age properly and SPB asymmetry is obliterated, thus explaining the loss of missegregation bias after the second cell cycle at restrictive temperature. It is worth noting that apparently contradictory data exist in the literature as to whether in *mps1* mutants chromosomes missegregate preferentially towards the bud (Araki et al., 2010; Jones et al., 2005; Maure et al., 2007). The above hypothesis offers a plausible explanation to reconcile these data.

Although the *mps1-3* Ser635Phe mutation lies in the kinase domain, the *in vitro* kinase activity of the corresponding protein is surprisingly enhanced, rather than impaired, at high temperature. The crystal structure of the Mps1 kinase domain has been solved (Chu et al., 2008) and reveals that Ser635 is semi-buried, thus precluding any straightforward prediction of the possible outcome of its mutation on Mps1 folding or activity. Importantly, the Mps1-3 protein does not accumulate at kinetochores, suggesting that lack of phosphorylation of specific kinetochore substrates underlies the chromosome biorientation and SAC defects of *mps1-3* cells. For what concerns SAC signalling, although *MPS1* overexpression is able to hyperactivate SAC in the absence of functional kinetochores (Fraschini et al., 2001a), our data

imply that endogenous levels of Mps1 must accumulate at kinetochores for a productive SAC response, in agreement with previous reports (Heinrich et al., 2012; Nijenhuis et al., 2013; Saurin et al., 2011; Zhu et al., 2013). Mps1 kinetochore recruitment depends on its N-terminus that interacts with the kinetochore protein Ndc80/Hec1 (Heinrich et al., 2012; Nijenhuis et al., 2013). Additionally, Mps1 kinase activity promotes its own turnover at kinetochores (Hewitt et al., 2010; Jelluma et al., 2010; Santaguida et al., 2010; Wang et al., 2014). It is therefore tempting to speculate that the enhanced kinase activity of Mps1-3 might accelerate its own turnover and account for its low levels at kinetochores. The characterisation of the intragenic suppressors identified in our genetic screen might help shedding light on this hypothesis.

Mps1 promotes SAC signalling and chromosome biorientation through a common molecular mechanism

Our unbiased screen for extragenic suppressors of *mps1-3* has been particularly revealing and points at the antagonism between Mps1 and PP1 at kinetochores as critical for the correction of faulty kinetochore-microtubule attachments and correct chromosome segregation. Our data strongly argue that the same mechanism implicated in SAC signalling, i.e. Spc105 phosphorylation and subsequent Bub1 recruitment, is a crucial function of Mps1 also in chromosome biorientation and independently of SAC activation. Several lines of evidence are consistent with this conclusion. First, the *spc105* and *GLC7* suppressors that we have identified can re-establish both proper chromosome segregation and SAC signalling in *mps1-3* cells without bringing back Mps1 to kinetochores. Second, Spc105 phosphorylation and Bub1 kinetochore localisation, which are severely impaired in *mps1-3* mutant cells, are restored in the suppressors. Third, constitutive binding of Bub1 to Spc105 is sufficient to rescue considerably chromosome missegregation and partly SAC signalling in *mps1-3* cells at

restrictive temperature. The incomplete rescue of SAC activation is not surprising, given that Mps1 plays additional roles in the SAC, such as promoting Bub1 and Mad1 phosphorylation (Ji et al., 2017; London and Biggins, 2014). Along this line, it is worth noting that the *spc105-18* and *GLC7-24* suppressors, which restore a normal SAC response in *mps1-3* cells, also restore wild type Mad1 (but not Bub1) hyperphosphorylation upon nocodazole treatment. The idea that a common molecular mechanism based on Knl1/Spc105 phosphorylation would underlie the role of Mps1 in both SAC and chromosome biorientation was previously proposed in fission yeast. Indeed, phospho-mimicking mutations in the MELT repeats of Spc7 (the fission yeast homologue of Knl1/Spc105) were shown to partially suppress the chromosome biorientation defects of *mps1Δ* cells (Yamagishi et al., 2012). However, in fission yeast Mps1 is not essential for viability, and *mps1Δ* cells experience only modest chromosome missegregation (Yamagishi et al., 2012). Thus, our data gathered in an organism where Mps1 is critical for chromosome biorientation and with the aid of an unbiased genetic screen largely extend and strengthen this idea.

The N-terminal region of Knl1 and Bub1 were previously shown to stimulate Aurora B kinase activity at kinetochores and increase the turnover of erroneous kinetochore-microtubule attachments (Caldas et al., 2013; Ricke et al., 2012, 2011). Furthermore, Bub1 has been involved in chromosome biorientation through phosphorylation of histone H2A and Sgo1 accumulation at pericentromeres (Fernius and Hardwick, 2007; Kawashima et al., 2010; Liu et al., 2015, 2013). Sgo1, in turn, enhances CPC activity in the error correction mechanism (Kawashima et al., 2007; Tsukahara et al., 2010; Verzijlbergen et al., 2014). Consistent with the idea that Mps1 is required for Bub1 recruitment to kinetochores, Sgo1 co-localisation with kinetochores is compromised in *mps1* mutants (Storchová et al., 2011 and our data). Our data suggest, however, that impaired Sgo1 kinetochore localisation does not fully account for the

chromosome biorientation defects of *mps1-3* cells. Indeed, Sgo1 centromeric recruitment is weakened, but not abolished, in *mps1-3* cells and the *mps1-3* mutation and *SGO1* deletion are synthetically lethal. Furthermore, mutations in the CPC centromere-targeting subunit Sli15 that rescue the sickness of *sgo1Δ* and *bub1Δ* cells (Campbell and Desai, 2013) have no ameliorating effects on the lethality and chromosome segregation defects of *mps1-3* cells at high temperature. Finally, phosphorylation of the Aurora B kinetochore target Dam1 is unaffected in *mps1-3* cells, suggesting that the error correction defects of this mutant are not caused by reduced Aurora B kinase activity. Thus, although Mps1 could promote chromosome biorientation partly through the Bub1-Sgo1-CPC axis, it must have at least one additional function in this process. Consistent with this hypothesis, Bub1 and Sgo1 are not essential proteins, unlike Mps1, and their deletion leads to milder chromosome segregation defects than *mps1-3* cells at restrictive temperature. One intriguing possibility that is supported by our genetic results is that Mps1 could directly harness PP1 activity at kinetochores. In this scenario, Mps1 would master two opposing activities, acting indirectly on the CPC and perhaps more directly on PP1, thereby allowing the highest accuracy of bipolar attachments. This hypothesis would also explain why the *spc105* and *GLC7* suppressors isolated in our screen rescue the lethality and chromosome segregation defects of *mps1-3* cells considerably better than artificial recruitment of Bub1 to Spc105. Whether and how Mps1 controls PP1 activity at kinetochores will be an important subject for future investigations.

In sum, our data provide experimental support to the hypothesis that a single sensory device may be used for both error correction of faulty kinetochore-microtubule attachments and SAC signalling (Caldas et al., 2013; Musacchio, 2011). Given the evolutionary conservation of the

players involved, it is very likely that Mps1 promotes SAC activation and chromosome biorientation through a common mechanism also in other organisms.

MATERIALS AND METHODS

Yeast strains, plasmids and growth conditions

All yeast strains (Table S1) are congenic to or at least four times backcrossed to W303 (*ade2-1, trp1-1, leu2-3,112, his3-11, and 15 ura3*).

One-step tagging techniques were used to generate 3HA-, 3PK-, GFP- and mCherry-tagged proteins at the C-terminus. The *CEN5::tetO2X224 (12,6Kb) tetR-GFP* strain was a generous gift from T. Tanaka (Tanaka et al., 2000); *BUB1-GFP* from P. de Wulf; *MTW1-Tomato* from A. Marston (Nerusheva et al., 2014); *GFP-TUB1* from A. Straight (Straight et al., 1997); *mCherry-TUB1* from A. Amon (Rock and Amon, 2011); *PDS1-myc18* from K. Nasmyth (Alexandru et al., 1999); *spc105-RASA* and *GLC7-spc105-RASA* mutants from H. Funabiki and F. Cross (Rosenberg et al., 2011); *SGO1-GFP* and *CEN5::tetO2X112* (1,4 Kb) *tetR-GFP* from E. Schwob; *ura3::URA3::tetOX224* (35Kb) *tetR-GFP* from K. Nasmyth. The *sli15-ΔNterm* (*sli15Δ2-228*) and *sli15-6A* plasmids (pCC253 and pCC297) were a gift of C. Campbell (Campbell and Desai, 2013) and were integrated at the *SLI15* locus by cutting with HindII and SalI respectively.

The *mps1-3* mutant was obtained by hydroxylamine-induced mutagenesis of an *MPS1*-bearing plasmid and selection of temperature-sensitive mutants through plasmid shuffling (Sikorski and Boeke, 1991). The *mps1-3* allele (entire coding sequence) together with 480 bp of 5' UTR and 900 bp of 3' UTR was cloned as an EcoRI/SalI fragment in the integrative plasmid pFL34 to generate pSP1041 and integrated at the *MPS1* locus by the Pop-in/Pop-out method (Scherer and Davis, 1979).

The *SPC105-GBD*-bearing plasmid (pSP1530) was generated by cloning in KpnI/HindIII of Yiplac204 a KpnI/PfoI fragment containing *SPC105* promoter and part of the coding region from plasmid SB1884 (London et al., 2012) together with a PfoI/HindIII *SPC105* synthetic

gene (aa 61-386 of Spc105) carrying the GBD domain after aa 130 (pSP1516). *SPC105-GBD* was integrated at the *SPC105* locus by digesting pSP1530 with BglII. This generates a partial duplication of *SPC105*, with full-length *SPC105-GBD* gene followed by a truncated *spc105* allele (aa 1-386).

The *GALs-MPS1* plasmid (pSP149) was constructed by amplifying a DNA fragment comprising 30 bp of *MPS1* 5' UTR, its CDS and 105 bp of 3' UTR by PCR from W303 genomic DNA with primers SP127 and SP129, followed by its cloning into EcoRI/XhoI of a pRS416 harbouring the attenuated *GALs* promoter (Mumberg et al., 1994). Growth of wild type cells carrying the *GALs-MPS1* construct is unaffected (data not shown), in contrast to high level overexpression of *MPS1* that causes a SAC-dependent metaphase arrest (Hardwick et al., 1996).

The *GAL1-GST-MPS1* plasmid (pSP228) was constructed by amplifying *MPS1* by PCR with primers SP239 and SP239 and cloning it into pEG(KT) (Pierce and Wendland, 2009) after cutting SmaI/HindIII. The *GAL1-GST-mps1-3* plasmid (pSP1202) was generated by replacing a BspEI/XbaI fragment of pSP228 internal to *MPS1* coding region by the same fragment containing the *mps1-3* mutation from pSP1041.

The plasmids for expression of His-tagged Mps1 and Mps1-3 in bacteria (pSP1575, pSP1576) were generated by amplifying the coding sequence of *MPS1/mps1-3* by PCR with primers MP1124-MP1125, followed by cloning into EcoRI/HindIII of pPROEX-HTa.

The plasmid for expression of His-tagged Spc105 N-terminus (aa 1-320) in *E. coli* (pSP1571) was generated by PCR-amplifying part of the coding sequence of *SPC105* with primers MP1126-1127, followed by cloning into BamHI/PstI of pPROEX-HTa.

Yeast cultures were grown at 25-30°C, in either SD medium (6.7 g/L yeast nitrogen base without aminoacids) supplemented with the appropriate nutrients or YEP (1% yeast extract, 2% bactopeptone, 50 mg/L adenine) medium. Raffinose was supplemented to 2% (SD-

raffinose or YEPR), glucose to 2% (SD-glucose or YEPD), and galactose to 1% (SD-raffinose/galactose or YEPRG). Cells were synchronized in G1 by alpha factor (4 μg/mL) in YEP medium containing the appropriate sugar at 25 °C. G1 arrest was monitored under a transmitted light microscope and cells were released in fresh medium (typically after 120–135 min of alpha factor treatment) at 34°C, unless otherwise specified, after being collected by centrifugation at 2000*g* followed by one wash with YEP containing the appropriate sugar. Nocodazole was used at 15 μg/mL.

Primers used in this study for gene tagging: Sequences in bold anneal to the tag-bearing cassette

SP84 (tagging *BUB1* with *3HA::K.l.URA3;* fwd)

ACGTAATTCTAAGCATTGAAGAGGAGTTATCACATTTTCAATATAAGGGGAAACC

GTCAAGGAGATTT**TCCGGTTCTGCTGCTAG**

SP85 (tagging *BUB1* with *3HA::K.l.URA3;* rev)

GTCATTGCTATGGAATCTGGCAGGACACCAAAAAGTCACCTATGCGGGAGATGA

AGGCATATTTATTCA**CCTCGAGGCCAGAAGAC**

SP96 (tagging *MPS1* with *3HA::K.l.URA3;* fwd)

CATATATCACAAGATGATCTCAATGATGTGGTAGACACTGTTTTAAGGAAATTTG

CAGATTACAAAATT**TCCGGTTCTGCTGCTAG**

SP97 (tagging *MPS1* with *3HA::K.l.URA3;* rev)

CATGCATGGCAAACTCTAAATGTATTTATGTTCATAACTGGCACATGCTTTTCTTC

CTTATGCGGCTCTT**CCTCGAGGCCAGAAGAC**

SP134 (tagging *MAD1* with *3HA::K.l.URA3;* fwd)

GATAGAGGTCAACTTCCGTGCTTTTTGGCAACAATAACATTGCGTCTGTGGGAAC

AGCGACAAGCCAAA**TCCGGTTCTGCTGCTAG**

SP135 (tagging *MAD1* with *3HA::K.l.URA3;* rev)

ATGTCAGCGGATAGGAGTTTATCATATTATAAAACCGATTACTATTATCTATTAG

AAATGTATATACAC**CCTCGAGGCCAGAAGAC**

MP560 (tagging *SPC97* with *mCherry::HPHMX*; fwd)

GTTCTTTACTCTATAGTACCTCCTCGCTCAGCATCTGCTTCTTCCCAAAGA**GGTCG**

ACGGATCCCCGGG

MP561 (tagging *SPC97* with *mCherry::HPHMX*; rev)

GATTCCACTTTCCGCAAGTTGGTGCACGTCGTTAGTGACATAACGCCGCGT**ATCG**

ATGAATTCGAGCTCG

MP629 (tagging *mps1-3* with *3HA::K.l.URA3;* fwd)

CTCAATGATGTGGTAGACACTGTTTTAAGGAAATTTGCAGATTACAAAATT**TCCG**

GTTCTGCTGCTAG

MP630 (tagging *mps1-3* with *3HA::K.l.URA3;* rev)

ATGTATTTATGTTCATAACTGGCACATGCTTTTCTTCCTTATGCGGCTCTT**CCTCG**

AGGCCAGAAGAC

MP761 (tagging *MPS1* with *6Gly-eGFP::kanMX* ; fwd)

CTCAATGATGTGGTAGACACTGTTTTAAGGAAATTTGCAGATTACAAAATTGGGG

GAGGCGGGGGTGGA**GGTGACGGTGCTGGTTTA**

MP762 (tagging *MPS1* with *6Gly-eGFP::kanMX* ; rev)

ATGTATTTATGTTCATAACTGGCACATGCTTTTCTTCCTTATGCGGCTCTT**TCGAT**

GAATTCGAGCTCG

MP763 (tagging *SPC105* with *3PK::K.l.HIS3;* fwd)

AGTGGAGTTCTTCCTTCATTTACGAAAAGTAGAATACATTTAGAGTTTACG**TCCG**

GTTCTGCTGCTAG

MP764 (tagging *SPC105* with *3PK::K.l.HIS3;* rev)

AAAAAAAAGTGATGAGATATTACTAGTCATCGTTGTCCTATTATAAACACT**CCTC**

GAGGCCAGAAGAC

MP894 (tagging *DAM1* with *3PK::K.l.HIS3;* fwd)

TCTGTTGCAAAGAAAACTGAAAAAAAAATAAATACAAGGCCCCCCTTCAGA**TCC**

GGTTCTGCTGCTAG

MP895 (tagging *DAM1* with *3PK::K.l.HIS3;* rev)

CTAGCGATATATTTTGTGAGGAGGATAATTCTTTGGTTGGGTTGGGCGTAG**CCTC**

GAGGCCAGAAGAC

MP900 (tagging *SNF1* with *3PK::K.l.HIS3;* fwd)

CATTTAACAACAAAACTAATTATGGAATTAGCCGTTAACAGTCAAAGCAAT**TCCG**

GTTCTGCTGCTAG

MP901 (tagging *SNF1* with *3PK::K.l.HIS3;* rev)

ACGATACATAAAAAAAAGGGAACTTCCATATCATTCTTTTACGTTCCACCA**CCTC**

GAGGCCAGAAGAC

MP940 (tagging *SLI15* with *3HA::K.l.URA3;* fwd)

AATCCTAGGCTAAACAGGTTGAAACCGCGTCAAATTGTGCCCAAAAGGTCT**TCC**

GGTTCTGCTGCTAG

MP941 (tagging *SLI15* with *3HA::K.l.URA3;* rev)

CTTGATTTAATGTTAACCAGTTTGAATTTTTCTTTTCTGGGGTAATCGAAT**CCTCG**

AGGCCAGAAGAC

MP1024 (tagging *BUB3* with *eGFP::kanMX*; fwd)

ACTATTGAACTAAACGCAAGTTCAATATACATAATATTTGACTATGAGAAC**GGG**

GGAGGCGGGGGTGGAGGTGACGGTGCTGGTTTA

MP1025 (tagging *BUB3* with *eGFP::kanMX*; rev)

AATTTTTTTTCTGGAATGTTCTATCATACTACACGAATCTTCACGAAGATA**TCGAT**

GAATTCGAGCTCG

MP1128 (tagging *MTW1* with *GBD::kanMX*; fwd)

GTTAGTATAGATATTGAAGAGCCTCAATTGGATTTACTTGATGATGTGTTA**CGTA**

CGCTGCAGGTCGAC

MP1129 (tagging *MTW1* with *GBD::kanMX*; rev)

ATTCGTGAATACATACATCATATCATAGCACATACTTTTTCCCACTTTATA**ATCGA**

TGAATTCGAGCTCG

Primers used in this study for cloning: sequences in bold indicate the restriction sites

SP127 (to clone *MPS1*, **EcoRI**)

CG**GAATTC**CTGCAAGAACTGGATGATCTC

SP129 (to clone *MPS1*, **XhoI**)

CCG**CTCGAG**CGGTGTAAAAAAGAGTTGATC

SP238 (cloning of *GAL1-GST-MPS1*; fwd)

TCCCCCGGGATCAACAAACTCATTCCATGATTAG

SP239 (cloning of *GAL1-GST-MPS1*; rev)

CCCAAGCTTAAGTATTCAGTGTCTGTGTCG

MP1124 (cloning of *MPS1*, **EcoRI**; fwd)

ACTTA**GAATTC**TCAACAAACTCATTCCATGATTATG

MP1125 (cloning of *MPS1*, **HindIII**; rev)

ACTTA**AAGCTT**CTAAATTTTGTAATCTGCAAATTTC

MP1126 (cloning N-ter SPC105, **BamHI**; fwd)

ACTTA**GGATCC**AATGTGGATGAAAGAAGCCG

MP1127 (cloning N-ter SPC105, **PstI**; rev)

ACTTA**CTGCAG**CTAGTCAAAGTTTGTCTGTATTTGCG

Microscopy

Scoring of GFP-tagged chromatid separation was carried out on cells fixed in 100% ethanol at -20°C. After two washes with PBS, cells were laid between a glass slide and a coverslip and imaged by fluorescence microscopy (Epifluorescent widefield Zeiss Axioimager Z1 controlled by the Metamorph software). Z-stacks (11 planes, 0.3 μm spaced) were max-projected before scoring.

To detect spindle formation and elongation, alpha-tubulin immunostaining was performed on formaldehyde-fixed cells using the YOL34 monoclonal antibody (1:100; MCA78S AbD Serotec, Raleigh, NC), followed by indirect immunofluorescence using CY2-conjugated anti-rat antibody (1:100; 31645 Pierce Chemical Co.).

For time-lapse video microscopy cells were mounted on 1% agarose pads in SD medium on Fluorodishes (World Precision Instruments) and filmed at controlled temperature with a 100X 1.45 NA oil immersion objective mounted on a Spinning disk CSU-X1 Andor Nikon Eclipse Ti microscope coupled to an iXon Ultra camera controlled by the Andor iQ3 software. Z stacks of 10 planes were acquired every 2-4 min with a step size of 0.5 µm (Fig. 1G, 3G, 4C, 5A), 0.3 µm (Fig S8A), or 0.67 µm (Fig S1A).

Images of Sgo1-GFP (Fig. S8A) have been deconvolved using the software Huygens using the following settings: background=200; ratio signal/noise=4; iterations=5.

Budding index was scored under a transmitted light microscope on cells fixed with 70% ethanol and treated for FACS analysis. Percentage of nuclear division was determined on the same samples after DNA staining with propidium iodide under a fluorescence microscope using a CY3 filter.

FACS analysis of DNA contents

For DNA quantification by fluorescence-activated cell sorting (FACS), 1–2 x 10^7 cells were collected, spun at 10000*g* and fixed with 1 mL of 70% ethanol for at least 30 min at RT. After one wash with 50 mM Tris-Cl pH 7.5, cells were resuspended in 0.5 mL of the same buffer containing 0.05 mL of a preboiled 10 mg/mL RNAse solution and incubated overnight at 37 °C. The next day cells were spun at 10,000g and resuspended in 0.5 mL of 5 mg/mL pepsin freshly diluted in in 55 mM HCl. After 30 min incubation at 37 °C cells were washed with FACS buffer (200 mM Tris-Cl pH 7.5, 200 mM NaCl, 78 mM $MgCl_2$) and resuspended in the same buffer containing 50 µg/mL propidium iodide. After a short sonication samples were diluted (1:20–1:10) in 1 mL of 50 mM Tris-Cl pH 7.5 and analysed with a FACSCalibur device (BD Biosciences). 10000 events were scored for each sample and plotted after gating out the debris.

Protein extracts, western blotting and kinase assays

For TCA protein extracts, 10–15 mL of cell culture in logarithmic phase (OD600 = 0.5-1) were collected by centrifugation at 2000*g*, washed with 1 mL of 20% TCA and resuspended in 100 µL of 20% TCA before breakage of cells with glass beads (diameter 0.5–0.75 mm) on a Vibrax VXR (IKA). After addition of 400 µL of 5% TCA, lysates were centrifuged for 10 min at 845*g*. Protein precipitates were resuspended in 100 µL of 3× SDS sample buffer (240 mM Tris-Cl pH6.8, 6% SDS, 30% glycerol, 2.28 M β-mercaptoethanol, 0.06% bromophenol blue), denatured at 99°C for 3 min and loaded on SDS-PAGE after elimination of cellular debris by centrifugation (5 min at 20000*g*).

Proteins were wet-transferred on Protran membranes (Schleicher and Schuell) overnight at 0.2 A and probed with: monoclonal anti-HA 12CA5 (1:5000); anti-PK (alias anti-V5; MCA1360 AbD Serotec, 1:3000); polyclonal anti-Cdc5 (sc-6733 Santa Cruz, 1:3000); anti-Clb2 (a

generous gift from W.Zachariae, 1:2000); anti-Pgk1 (Invitrogen Molecular Probes, 1:40000); monoclonal anti-myc 9E10 (1:5000); anti-phospho-AMPK (Thr172) (Cell Signalling, 1:1000); anti-GST (1:2000, 27-4577-01 GE Healthcare). Antibodies were diluted in 5% low-fat milk (Regilait) dissolved in TBST. Secondary antibodies were purchased from GE Healthcare and proteins were detected by a home-made enhanced chemiluminescence system. For kinase assays with recombinant Mps1 proteins, Mps1/Mps1-3 and Spc105 have been purified as follows: BL21 DE3 cells transformed with pSP1571, pSP1575 or pSP1576 were grown in LB containing 50µg/mL of ampicillin, 34µg/mL of cloramphenicol and 1% glucose and induced with 0.2 mM IPTG at 16°C overnight. Cells were lysed in 50mM Tris-Cl pH 8, 300mM NaCl, 0.1% Tween20 containing 1mg/mL of lysozyme and a cocktail of protease inhibitors (Complete EDTA-free Roche). Cells were then sonicated 3x with 1'30'' cycles of 8'' pulses/8'' ice and extracts cleared at 30000*g* for 30' at 4°C. Lysates were incubated 2h with 1mL of Ni-NTA agarose beads (Qiagen), pre-washed 3 times with 50mM Tris-Cl pH 8, 300mM NaCl, 0.1% Tween20, 10mM imidazole at 4°C. After incubation with the extracts, the slurry was washed 3 times with 50mM Tris-Cl pH 8, 300mM NaCl, 0.1% Tween20, 20mM imidazole and loaded on Polyprep columns (BioRad). Fractions of 0.5mL were eluted with 50mM Tris-Cl pH 8, 300mM NaCl 250mM imidazole and quantified by Nanodrop. The most concentrated fractions were washed and concentrated through the use of Amicon Ultra filter units (10 KDa cut-off for Spc105 and 50 KDa cut-off for Mps1) to finally have them in 50mM Tris-Cl pH 8, 50mM NaCl. Glycerol was added to the final concentration of 20%. Protein concentration was quantified by loading them on SDS-page along with a BSA standard curve followed by staining with Coomassie blue. Kinase assays were performed at 34°C for different times in 20 µL of a reaction mix containing 50mM Tris-Cl pH7.5, 10mM $MgCl_2$, 0.5mM DTT, 10µM ATP, 1 µL ATP-γ^{P33} 3000 Ci/mmol, 80µg/mL MBP. 75 ng of Spc105 N-term fragment and 1µg Mps1/Mps1-3 kinases were used for each assay. Reactions

were stopped using 7 µL of 3x SDS sample buffer (described in TCA extracts). Samples were then boiled 3 minutes at 95°C and loaded on SDS-PAGE. The gel was then dried and exposed on autoradiography films.

Native yeast protein extracts for kinase assays were performed by collecting cells in logarithmic phase (OD_{600} = 1) grown in -Ura RG at 30°C, centrifuging at 2000*g* and washing with 1 mL of cold 10 mM Tris-Cl pH 7.5. Cells were then broken in 50mM Tris-Cl pH 7.5, 50mM NaCl, 0.2% TritonX100 containing a cocktail of protease inhibitors (Complete EDTA-free Roche) and phosphatase inhibitors (PhosSTOP Roche). Lysates were cleared at 20000*g* for 10 min at 4 °C. The equivalent of 6 OD_{600}/assay was incubated on a nutator for 2h at 4 °C with 50 µL of Glutathione Sepharose 4 Fast Flow (GE Healthcare) beads pre-washed with the above buffer. After incubation with the extracts, beads were spun down at 4°C at 845*g*, washed twice with the same buffer without protease and phosphatase inhibitors, twice with the same buffer containing 0.1% of Triton X100, twice with the same buffer without Triton X100 and once with 50mM Tris-Cl pH 7.5, 10mM $MgCl_2$, 0.5mM DTT. Kinase assays were performed as above using 2 µg of MBP as exogenous substrate.

Chromosome loss assay

This assay is based on the loss of heterozygosity of the *MAT* locus, carried by chromosome III (Andersen et al., 2008). Briefly, wild type diploid cells are heterozygous *MATa/MATalpha* and cannot mate unless they lose one copy of the *MAT* locus through mutations, chromosome re-arrangements or chromosome loss. Cells were grown overnight at 25°C and their concentration was measured at the time of inoculation and the day after to calculate the number of cell divisions. $2x10^7$ diploid Met^+ cells were incubated 4 hours at RT with an excess ($2x10^8$) MATalpha *met4* tester cells in 400 µL of YEPD. 10 µL of the suspension was then diluted to plate 500 cells on –Met plates (where only the Met^+ diploids can form

colonies) to calculate the percentage of viable (i.e. colony-forming); the remaining cells were plated on minimal SD plates (MIN), where only triploids, generated from the mating of diploids with the haploid tester cells, can grow. Plates have been incubated at 25°C. Frequency of chromosome loss has been calculated as follows: {[(n° of colonies on MIN / $2x10^7$) / fraction of viable cells] / n° of cellular divisions}. We note that with this assay we likely underestimate the real frequencies of chromosome loss because our measurements do not take into account the frequency of mating for each strain, which probably is much lower than 100%.

Suppressor screen

$2.6x10^7$ *mps1-3* cells were plated on YEPD and incubated at 34°C for 3-5 days until colonies appearance. The isolated spontaneous suppressors were then characterised by classical genetic tests to distinguish intragenic from extragenic mutations, recessive from dominant mutations, and to group the suppressors in complementation/allelic groups. Genomic DNA was extracted from one representative suppressor for each complementation/allelic group and sent for whole genome sequencing to identify the mutated genes. The identity of the suppressing mutations was confirmed by classical genetics. Targeted gene re-sequencing approaches were used to identify the supressing mutations in the other extragenic suppressors.

Viability test

Cells were grown at 25°C to $2x10^6$ cells/mL and then serially diluted to plate 200 cells/plate in duplicate (wild type, *mps1-3 SPC105-GBD BUB1-GFP* and *mps1-3 SPC105-GBD BUB3-GFP*) or 200, 500 and 1000 cells/plate in duplicate for *mps1-3* cells (t=0). Cells were then shifted to 34°C, withdrawn each hour, serially diluted to plate 200 cells/plate in duplicate (wild type, *mps1-3 SPC105-GBD BUB1-GFP* and *mps1-3 SPC105-GBD BUB3-GFP*) or 200,

500 and 1000 cells/plate in duplicate for *mps1-3* cells. Plates were incubated at 25°C until colony appearance. The number of colonies at each time point (average values of the duplicates) was divided by the number of colonies at t=0 to obtain percentages of viability.

ChIP-seq analysis

100 mL of cells (concentration 10^7cells/mL) were fixed in 1% formaldehyde for 30' at RT with shaking and then transferred ON at 4°C. Cells were then spun down 3min at 3000 rpm at 4°C and washed three times with TBS. Cells were resuspended in 0.4 mL of 50mM Hepes-KOH pH7.5, 140mM NaCl, 1mM EDTA, 1% Triton-X100, 0.1% Na-deoxicholate containing a cocktail of protease inhibitors (Complete EDTA-free Roche) and 1mM PMSF, followed by cell breakage through a Multi-beads shaker (Yasui-Kikai) at 0°C. Lysates were eluted in 15mL Falcon tubes (centrifuged twice at 3000 rpm for 1 min at 4°C), transferred in 1.5 Eppendorf tube, centrifuged at 5000 rpm 1 min at 4°C and sonicated through a Sonifyer Branson 2508 (5-7 cycles of 15sec, tune 1.5 with centrifugation of 5000 rpm for 1 min between each cycle). Sonicated lysates were then centrifuged for 5 min at 15000 rpm at 4°C. Supernatants were recovered. 10 µL of lysates were withdrawn at this stage (=Inputs). For immunoprecipitations (IPs), 60 µL of Protein G-dynabeads pre-washed twice with PBS containing 5 mg/mL BSA and pre-adsorbed with 3 µg Babco 16B12 anti-HA antibody were added to each lysate and incubated ON at 4°C on a nutator. IPs were then washed twice with ice-cold 50mM Hepes-KOH pH7.5, 140mM NaCl, 1mM EDTA, 1% Triton-X100, 0.1% Na-deoxicholate, twice with ice-cold 50mM Hepes-KOH pH7.5, 500mM NaCl, 1mM EDTA, 1% Triton-X100, 0.1% Na-deoxicholate, twice with ice-cold 10mM Tris-Cl pH8, 250mM LiCl, 0.5% NP-40, 0.5% Na-deoxycholate, 1mM EDTA and once with ice-cold TE (50mM Tris-Cl pH8, 1mM EDTA pH8). IPs were eluted at 65°C for 15min with 50µL of 50mM Tris-Cl pH8, 10mM EDTA, 1% SDS, resuspended in 50 µL of TE/1% SDS and incubated overnight at

65°C to reverse crosslinking. IPs were then incubated at 37°C for 1 hour with 100 µL of TE containing 10 µg of RNAseA and 2 hours at 37°C with 2 µL of ProteinaseK 50 mg/mL. DNA was then purified with the Qiagen PCR purification kit. Libraries for Illumina sequencing have been then prepared following the NEBNext Ultra II DNA Library Prep Kit for Illumina. Sequencing results have been analysed using the DROMPA software (Nakato and Shirahige, 2018).

ACKNOWLEDGMENTS

We are grateful to P. Pietruszka for initial experiments on *mps1-3*; to A. Amon, S. Biggins, C. Campbell, F. Cross, A. Desai, P. De Wulf, H. Funabiki, A. Hoyt, A. Marston, K. Nasmyth, E. Schwob, S. Storchova, A. Straight, T. Tanaka, W. Zachariae for sharing reagents; to K. Fujiki for analysis of ChIP-seq data; to V. Georget, S. De Rossi and O. Faklaris for their invaluable help with live cell imaging; to A. Musacchio and E. Schwob for insightful suggestions; to members of S. Piatti's lab for useful discussions; to A. Musacchio and A. Abrieu for critical reading of the manuscript. We acknowledge the imaging core facility MRI, member of the national infrastructure France-BioImaging supported by the French National Research Agency (ANR-10-INBS-04, "Investments for the future"). This work has been supported by the Fondation pour la Recherche Médicale (DEQ20150331740 to S.P.) and by Labex EpiGenMed (PhD fellowship to G.B.). The authors declare no competing interests.

REFERENCES

Alexandru G, Zachariae W, Schleiffer A, Nasmyth K. 1999. Sister chromatid separation and chromosome re-duplication are regulated by different mechanisms in response to spindle damage. *Embo J* **18**:2707–21.

Andersen MP, Nelson ZW, Hetrick ED, Gottschling DE. 2008. A Genetic Screen for Increased Loss of Heterozygosity in Saccharomyces cerevisiae. *Genetics* **179**:1179–1195. doi:10.1534/genetics.108.089250

Angus-Hill ML, Schlichter A, Roberts D, Erdjument-Bromage H, Tempst P, Cairns BR. 2001. A Rsc3/Rsc30 zinc cluster dimer reveals novel roles for the chromatin remodeler RSC in gene expression and cell cycle control. *Mol Cell* **7**:741–751.

Araki Y, Gombos L, Migueleti SPS, Sivashanmugam L, Antony C, Schiebel E. 2010. N-terminal regions of Mps1 kinase determine functional bifurcation. *J Cell Biol* **189**:41–56. doi:10.1083/jcb.200910027

Aravamudhan P, Goldfarb AA, Joglekar AP. 2015. The kinetochore encodes a mechanical switch to disrupt spindle assembly checkpoint signalling. *Nat Cell Biol* **17**:868–879. doi:10.1038/ncb3179

Bloom K, Yeh E. 2010. Tension Management in the Kinetochore. *Curr Biol* **20**:R1040–R1048. doi:10.1016/j.cub.2010.10.055

Bokros M, Gravenmier C, Jin F, Richmond D, Wang Y. 2016. Fin1-PP1 Helps Clear Spindle Assembly Checkpoint Protein Bub1 from Kinetochores in Anaphase. *Cell Reports* **14**:1074–1085. doi:10.1016/j.celrep.2016.01.007

Breit C, Bange T, Petrovic A, Weir JR, Müller F, Vogt D, Musacchio A. 2015. Role of Intrinsic and Extrinsic Factors in the Regulation of the Mitotic Checkpoint Kinase Bub1. *PLOS ONE* **10**:e0144673. doi:10.1371/journal.pone.0144673

Caldas GV, DeLuca KF, DeLuca JG. 2013. KNL1 facilitates phosphorylation of outer kinetochore proteins by promoting Aurora B kinase activity. *J Cell Biol* **203**:957–969. doi:10.1083/jcb.201306054

Campbell CS, Desai A. 2013. Tension sensing by Aurora B kinase is independent of survivin-based centromere localization. *Nature* **497**:118–121. doi:10.1038/nature12057

Carmena M, Wheelock M, Funabiki H, Earnshaw WC. 2012. The chromosomal passenger complex (CPC): from easy rider to the godfather of mitosis. *Nature Reviews Molecular Cell Biology* **13**:789–803. doi:10.1038/nrm3474

Cheeseman IM, Anderson S, Jwa M, Green EM, Kang J, Yates JR, Chan CSM, Drubin DG, Barnes G. 2002. Phospho-Regulation of Kinetochore-Microtubule Attachments by the Aurora Kinase Ipl1p. *Cell* **111**:163–172. doi:10.1016/S0092-8674(02)00973-X

Chu MLH, Chavas LMG, Douglas KT, Eyers PA, Tabernero L. 2008. Crystal structure of the catalytic domain of the mitotic checkpoint kinase Mps1 in complex with SP600125. *J Biol Chem* **283**:21495–21500. doi:10.1074/jbc.M803026200

Ditchfield C, Johnson VL, Tighe A, Ellston R, Haworth C, Johnson T, Mortlock A, Keen N, Taylor SS. 2003. Aurora B couples chromosome alignment with anaphase by targeting BubR1, Mad2, and Cenp-E to kinetochores. *J Cell Biol* **161**:267–80.

Fernius J, Hardwick KG. 2007. Bub1 kinase targets Sgo1 to ensure efficient chromosome biorientation in budding yeast mitosis. *PLoS Genet* **3**:e213.

Fischböck-Halwachs J, Singh S, Potocnjak M, Hagemann G, Solis-Mezarino V, Woike S, Ghodgaonkar-Steger M, Weissmann F, Gallego LD, Rojas J, Andreani J, Köhler A, Herzog F. 2019. The COMA complex interacts with Cse4 and positions Sli15/Ipl1 at the budding yeast inner kinetochore. *eLife* **8**. doi:10.7554/eLife.42879

Fischboeck J, Singh S, Potocnjak M, Hagemann G, Solis V, Woike S, Ghodgaonkar M, Andreani J, Herzog F. 2018. The COMA complex is required for positioning Ipl1 activity proximal to Cse4 nucleosomes in budding yeast. *bioRxiv*. doi:10.1101/444570

Fischer MG, Heeger S, Häcker U, Lehner CF. 2004. The mitotic arrest in response to hypoxia and of polar bodies during early embryogenesis requires Drosophila Mps1. *Curr Biol* **14**:2019–2024. doi:10.1016/j.cub.2004.11.008

Francisco L, Wang W, Chan CS. 1994. Type 1 protein phosphatase acts in opposition to IpL1 protein kinase in regulating yeast chromosome segregation. *Mol Cell Biol* **14**:4731–4740.

Fraschini R, Beretta A, Lucchini G, Piatti S. 2001a. Role of the kinetochore protein Ndc10 in mitotic checkpoint activation in Saccharomyces cerevisiae. *Mol Genet Genomics* **266**:115–25.

Fraschini R, Beretta A, Sironi L, Musacchio A, Lucchini G, Piatti S. 2001b. Bub3 interaction with Mad2, Mad3 and Cdc20 is mediated by WD40 repeats and does not require intact kinetochores. *Embo J* **20**:6648–59.

García-Rodríguez LJ, Kasciukovic T, Denninger V, Tanaka TU. 2019. Aurora B-INCENP Localization at Centromeres/Inner Kinetochores Is Required for Chromosome Bi-orientation in Budding Yeast. *Current Biology* **29**:1536-1544.e4. doi:10.1016/j.cub.2019.03.051

Gillett ES, Espelin CW, Sorger PK. 2004. Spindle checkpoint proteins and chromosome-microtubule attachment in budding yeast. *J Cell Biol* **164**:535–46.

Hardwick KG, Murray AW. 1995. Mad1p, a phosphoprotein component of the spindle assembly checkpoint in budding yeast. *J Cell Biol* **131**:709–20.
Hardwick KG, Weiss E, Luca FC, Winey M, Murray AW. 1996. Activation of the budding yeast spindle assembly checkpoint without mitotic spindle disruption. *Science* **273**:953–6.
Hauf S, Cole RW, LaTerra S, Zimmer C, Schnapp G, Walter R, Heckel A, van Meel J, Rieder CL, Peters JM. 2003. The small molecule Hesperadin reveals a role for Aurora B in correcting kinetochore-microtubule attachment and in maintaining the spindle assembly checkpoint. *J Cell Biol* **161**:281–94.
Hayward D, Bancroft J, Mangat D, Alfonso-Pérez T, Dugdale S, McCarthy J, Barr FA, Gruneberg U. 2019. Checkpoint signaling and error correction require regulation of the MPS1 T-loop by PP2A-B56. *The Journal of Cell Biology* jcb.201905026. doi:10.1083/jcb.201905026
Heinrich S, Windecker H, Hustedt N, Hauf S. 2012. Mph1 kinetochore localization is crucial and upstream in the hierarchy of spindle assembly checkpoint protein recruitment to kinetochores. *J Cell Sci* **125**:4720–4727. doi:10.1242/jcs.110387
Hewitt L, Tighe A, Santaguida S, White AM, Jones CD, Musacchio A, Green S, Taylor SS. 2010. Sustained Mps1 activity is required in mitosis to recruit O-Mad2 to the Mad1-C-Mad2 core complex. *J Cell Biol* **190**:25–34. doi:10.1083/jcb.201002133
Hoyt MA, Totis L, Roberts BT. 1991. S. cerevisiae genes required for cell cycle arrest in response to loss of microtubule function. *Cell* **66**:507–17.
Hsu JY, Sun ZW, Li X, Reuben M, Tatchell K, Bishop DK, Grushcow JM, Brame CJ, Caldwell JA, Hunt DF, Lin R, Smith MM, Allis CD. 2000. Mitotic phosphorylation of histone H3 is governed by Ipl1/aurora kinase and Glc7/PP1 phosphatase in budding yeast and nematodes. *Cell* **102**:279–291.
Indjeian VB, Stern BM, Murray AW. 2005. The centromeric protein Sgo1 is required to sense lack of tension on mitotic chromosomes. *Science* **307**:130–133. doi:10.1126/science.1101366
Irniger S, Piatti S, Michaelis C, Nasmyth K. 1995. Genes involved in sister chromatid separation are needed for B-type cyclin proteolysis in budding yeast [published erratum appears in Cell 1998 May 1;93(3):487]. *Cell* **81**:269–78.
Jelluma N, Brenkman AB, van den Broek NJF, Cruijsen CWA, van Osch MHJ, Lens SMA, Medema RH, Kops GJPL. 2008. Mps1 phosphorylates Borealin to control Aurora B activity and chromosome alignment. *Cell* **132**:233–246. doi:10.1016/j.cell.2007.11.046
Jelluma N, Dansen TB, Sliedrecht T, Kwiatkowski NP, Kops GJPL. 2010. Release of Mps1 from kinetochores is crucial for timely anaphase onset. *The Journal of Cell Biology* **191**:281–290. doi:10.1083/jcb.201003038
Ji Z, Gao H, Jia L, Li B, Yu H. 2017. A sequential multi-target Mps1 phosphorylation cascade promotes spindle checkpoint signaling. *eLife* **6**. doi:10.7554/eLife.22513
Jones MH, Huneycutt BJ, Pearson CG, Zhang C, Morgan G, Shokat K, Bloom K, Winey M. 2005. Chemical genetics reveals a role for Mps1 kinase in kinetochore attachment during mitosis. *Curr Biol* **15**:160–165. doi:10.1016/j.cub.2005.01.010
Kalantzaki M, Kitamura E, Zhang T, Mino A, Novák B, Tanaka TU. 2015. Kinetochore–microtubule error correction is driven by differentially regulated interaction modes. *Nature Cell Biology* **17**:421–433. doi:10.1038/ncb3128
Kallio MJ, McCleland ML, Stukenberg PT, Gorbsky GJ. 2002. Inhibition of aurora B kinase blocks chromosome segregation, overrides the spindle checkpoint, and perturbs microtubule dynamics in mitosis. *Curr Biol* **12**:900–5.
Kawashima SA, Tsukahara T, Langegger M, Hauf S, Kitajima TS, Watanabe Y. 2007. Shugoshin enables tension-generating attachment of kinetochores by loading Aurora to centromeres. *Genes Dev* **21**:420–435. doi:10.1101/gad.1497307
Kawashima SA, Yamagishi Y, Honda T, Ishiguro K, Watanabe Y. 2010. Phosphorylation of H2A by Bub1 prevents chromosomal instability through localizing shugoshin. *Science* **327**:172–177. doi:10.1126/science.1180189
Kim J, Kang J, Chan CSM. 1999. Sli15 Associates with the Ipl1 Protein Kinase to Promote Proper Chromosome Segregation in Saccharomyces cerevisiae. *J Cell Biol* **145**:1381–1394.
King EMJ, Rachidi N, Morrice N, Hardwick KG, Stark MJR. 2007. Ipl1p-dependent phosphorylation of Mad3p is required for the spindle checkpoint response to lack of tension at kinetochores. *Genes Dev* **21**:1163–1168. doi:10.1101/gad.431507
Krenn V, Musacchio A. 2015. The Aurora B Kinase in Chromosome Bi-Orientation and Spindle Checkpoint Signaling. *Frontiers in oncology* **5**:225. doi:10.3389/fonc.2015.00225
Lampson MA, Grishchuk EL. 2017. Mechanisms to Avoid and Correct Erroneous Kinetochore-Microtubule Attachments. *Biology (Basel)* **6**. doi:10.3390/biology6010001
Lauzé E, Stoelcker B, Luca FC, Weiss E, Schutz AR, Winey M. 1995. Yeast spindle pole body duplication gene MPS1 encodes an essential dual specificity protein kinase. *EMBO J* **14**:1655–1663.
Li R, Murray AW. 1991. Feedback control of mitosis in budding yeast. *Cell* **66**:519–31.

Liu D, Vleugel M, Backer CB, Hori T, Fukagawa T, Cheeseman IM, Lampson MA. 2010. Regulated targeting of protein phosphatase 1 to the outer kinetochore by KNL1 opposes Aurora B kinase. *The Journal of Cell Biology* **188**:809–820. doi:10.1083/jcb.201001006

Liu H, Jia L, Yu H. 2013. Phospho-H2A and cohesin specify distinct tension-regulated Sgo1 pools at kinetochores and inner centromeres. *Curr Biol* **23**:1927–1933. doi:10.1016/j.cub.2013.07.078

Liu H, Qu Q, Warrington R, Rice A, Cheng N, Yu H. 2015. Mitotic Transcription Installs Sgo1 at Centromeres to Coordinate Chromosome Segregation. *Mol Cell* **59**:426–436. doi:10.1016/j.molcel.2015.06.018

London N, Biggins S. 2014. Mad1 kinetochore recruitment by Mps1-mediated phosphorylation of Bub1 signals the spindle checkpoint. *Genes Dev* **28**:140–152. doi:10.1101/gad.233700.113

London N, Ceto S, Ranish JA, Biggins S. 2012. Phosphoregulation of Spc105 by Mps1 and PP1 Regulates Bub1 Localization to Kinetochores. *Current Biology* **22**:900–906. doi:10.1016/j.cub.2012.03.052

Maciejowski J, Drechsler H, Grundner-Culemann K, Ballister ER, Rodriguez-Rodriguez J-A, Rodriguez-Bravo V, Jones MJK, Foley E, Lampson MA, Daub H, McAinsh AD, Jallepalli PV. 2017. Mps1 Regulates Kinetochore-Microtubule Attachment Stability via the Ska Complex to Ensure Error-Free Chromosome Segregation. *Developmental Cell* **41**:143-156.e6. doi:10.1016/j.devcel.2017.03.025

Makrantoni V, Stark MJR. 2009. Efficient Chromosome Biorientation and the Tension Checkpoint in Saccharomyces cerevisiae both Require Bir1. *Molecular and Cellular Biology* **29**:4552–4562. doi:10.1128/MCB.01911-08

Maldonado M, Kapoor TM. 2011. Constitutive Mad1 targeting to kinetochores uncouples checkpoint signalling from chromosome biorientation. *Nat Cell Biol* **13**:475–482. doi:10.1038/ncb2223

Maure JF, Kitamura E, Tanaka TU. 2007. Mps1 kinase promotes sister-kinetochore bi-orientation by a tension-dependent mechanism. *Curr Biol* **17**:2175–82.

Meadows JC, Shepperd LA, Vanoosthuyse V, Lancaster TC, Sochaj AM, Buttrick GJ, Hardwick KG, Millar JBA. 2011. Spindle checkpoint silencing requires association of PP1 to both Spc7 and kinesin-8 motors. *Dev Cell* **20**:739–750. doi:10.1016/j.devcel.2011.05.008

Michaelis C, Ciosk R, Nasmyth K. 1997. Cohesins: chromosomal proteins that prevent premature separation of sister chromatids. *Cell* **91**:35–45.

Mora-Santos MDM, Hervas-Aguilar A, Sewart K, Lancaster TC, Meadows JC, Millar JBA. 2016. Bub3-Bub1 Binding to Spc7/KNL1 Toggles the Spindle Checkpoint Switch by Licensing the Interaction of Bub1 with Mad1-Mad2. *Curr Biol* **26**:2642–2650. doi:10.1016/j.cub.2016.07.040

Moura M, Osswald M, Leça N, Barbosa J, Pereira AJ, Maiato H, Sunkel CE, Conde C. 2017. Protein Phosphatase 1 inactivates Mps1 to ensure efficient Spindle Assembly Checkpoint silencing. *eLife* **6**. doi:10.7554/eLife.25366

Moyle MW, Kim T, Hattersley N, Espeut J, Cheerambathur DK, Oegema K, Desai A. 2014. A Bub1–Mad1 interaction targets the Mad1–Mad2 complex to unattached kinetochores to initiate the spindle checkpoint. *J Cell Biol* **204**:647–657. doi:10.1083/jcb.201311015

Mumberg D, Muller R, Funk M. 1994. Regulatable promoters of Saccharomyces cerevisiae: comparison of transcriptional activity and their use for heterologous expression. *Nucleic Acids Res* **22**:5767–8.

Musacchio A. 2015. The Molecular Biology of Spindle Assembly Checkpoint Signaling Dynamics. *Current Biology* **25**:R1002–R1018. doi:10.1016/j.cub.2015.08.051

Musacchio A. 2011. Spindle assembly checkpoint: the third decade. *Philos Trans R Soc Lond, B, Biol Sci* **366**:3595–3604. doi:10.1098/rstb.2011.0072

Nakajima Y, Cormier A, Tyers RG, Pigula A, Peng Y, Drubin DG, Barnes G. 2011. Ipl1/Aurora-dependent phosphorylation of Sli15/INCENP regulates CPC–spindle interaction to ensure proper microtubule dynamics. *The Journal of Cell Biology* **194**:137–153. doi:10.1083/jcb.201009137

Nakato R, Shirahige K. 2018. Statistical Analysis and Quality Assessment of ChIP-seq Data with DROMPA. *Genome Instability* 631–643. doi:10.1007/978-1-4939-7306-4_41

Nerusheva OO, Galander S, Fernius J, Kelly D, Marston AL. 2014. Tension-dependent removal of pericentromeric shugoshin is an indicator of sister chromosome biorientation. *Genes Dev* **28**:1291–1309. doi:10.1101/gad.240291.114

Nijenhuis W, von Castelmur E, Littler D, De Marco V, Tromer E, Vleugel M, van Osch MHJ, Snel B, Perrakis A, Kops GJPL. 2013. A TPR domain-containing N-terminal module of MPS1 is required for its kinetochore localization by Aurora B. *J Cell Biol* **201**:217–231. doi:10.1083/jcb.201210033

Palframan WJ, Meehl JB, Jaspersen SL, Winey M, Murray AW. 2006. Anaphase inactivation of the spindle checkpoint. *Science* **313**:680–4.

Peplowska K, Wallek AU, Storchova Z. 2014. Sgo1 Regulates Both Condensin and Ipl1/Aurora B to Promote Chromosome Biorientation. *PLOS Genetics* **10**:e1004411. doi:10.1371/journal.pgen.1004411

Pereira G, Schiebel E. 2003. Separase regulates INCENP-Aurora B anaphase spindle function through Cdc14. *Science* **302**:2120–4.

Petersen J, Hagan IM. 2003. S. pombe Aurora Kinase/Survivin Is Required for Chromosome Condensation and

the Spindle Checkpoint Attachment Response. *Curr Biol* **13**:590–7.
Pierce BD, Wendland B. 2009. Sequence of the yeast protein expression plasmid pEG(KT). *Yeast* **26**:349–353. doi:10.1002/yea.1667
Pinsky BA, Kung C, Shokat KM, Biggins S. 2006. The Ipl1-Aurora protein kinase activates the spindle checkpoint by creating unattached kinetochores. *Nat Cell Biol* **8**:78–83. doi:10.1038/ncb1341
Pinsky BA, Nelson CR, Biggins S. 2009. Protein Phosphatase 1 Regulates Exit from the Spindle Checkpoint in Budding Yeast. *Curr Biol*. doi:10.1016/j.cub.2009.06.043
Primorac I, Weir JR, Chiroli E, Gross F, Hoffmann I, van Gerwen S, Ciliberto A, Musacchio A. 2013. Bub3 reads phosphorylated MELT repeats to promote spindle assembly checkpoint signaling. *eLife* **2**:e01030. doi:10.7554/eLife.01030
Ricke RM, Jeganathan KB, Malureanu L, Harrison AM, van Deursen JM. 2012. Bub1 kinase activity drives error correction and mitotic checkpoint control but not tumor suppression. *The Journal of Cell Biology* **199**:931–949. doi:10.1083/jcb.201205115
Ricke RM, Jeganathan KB, van Deursen JM. 2011. Bub1 overexpression induces aneuploidy and tumor formation through Aurora B kinase hyperactivation. *J Cell Biol* **193**:1049–1064. doi:10.1083/jcb.201012035
Rivera T, Ghenoiu C, Rodríguez-Corsino M, Mochida S, Funabiki H, Losada A. 2012. Xenopus Shugoshin 2 regulates the spindle assembly pathway mediated by the chromosomal passenger complex: XSgo2 regulates the spindle assembly pathway mediated by CPC. *The EMBO Journal* **31**:1467–1479. doi:10.1038/emboj.2012.4
Roberts BT, Farr KA, Hoyt MA. 1994. The Saccharomyces cerevisiae checkpoint gene BUB1 encodes a novel protein kinase. *Mol Cell Biol* **14**:8282–91.
Rock JM, Amon A. 2011. Cdc15 integrates Tem1 GTPase-mediated spatial signals with Polo kinase-mediated temporal cues to activate mitotic exit. *Genes & development* **25**:1943–54. doi:10.1101/gad.17257711
Rosenberg JS, Cross FR, Funabiki H. 2011. KNL1/Spc105 recruits PP1 to silence the spindle assembly checkpoint. *Curr Biol* **21**:942–947. doi:10.1016/j.cub.2011.04.011
Rothbauer U, Zolghadr K, Muyldermans S, Schepers A, Cardoso MC, Leonhardt H. 2008. A versatile nanotrap for biochemical and functional studies with fluorescent fusion proteins. *Mol Cell Proteomics* **7**:282–9. doi:10.1074/mcp.M700342-MCP200
Rubenstein EM, McCartney RR, Zhang C, Shokat KM, Shirra MK, Arndt KM, Schmidt MC. 2008. Access Denied: Snf1 Activation Loop Phosphorylation Is Controlled by Availability of the Phosphorylated Threonine 210 to the PP1 Phosphatase. *J Biol Chem* **283**:222–230. doi:10.1074/jbc.M707957200
Santaguida S, Tighe A, D'Alise AM, Taylor SS, Musacchio A. 2010. Dissecting the role of MPS1 in chromosome biorientation and the spindle checkpoint through the small molecule inhibitor reversine. *J Cell Biol* **190**:73–87. doi:10.1083/jcb.201001036
Santaguida S, Vernieri C, Villa F, Ciliberto A, Musacchio A. 2011. Evidence that Aurora B is implicated in spindle checkpoint signalling independently of error correction. *EMBO J* **30**:1508–1519. doi:10.1038/emboj.2011.70
Saurin AT, van der Waal MS, Medema RH, Lens SMA, Kops GJPL. 2011. Aurora B potentiates Mps1 activation to ensure rapid checkpoint establishment at the onset of mitosis. *Nat Commun* **2**:316. doi:10.1038/ncomms1319
Scherer S, Davis RW. 1979. Replacement of chromosome segments with altered DNA sequences constructed in vitro. *Proc Natl Acad Sci USA* **76**:4951–4955.
Shepperd LA, Meadows JC, Sochaj AM, Lancaster TC, Zou J, Buttrick GJ, Rappsilber J, Hardwick KG, Millar JBA. 2012. Phosphodependent recruitment of Bub1 and Bub3 to Spc7/KNL1 by Mph1 kinase maintains the spindle checkpoint. *Curr Biol* **22**:891–899. doi:10.1016/j.cub.2012.03.051
Shimogawa MM, Graczyk B, Gardner MK, Francis SE, White EA, Ess M, Molk JN, Ruse C, Niessen S, Yates JR, Muller EGD, Bloom K, Odde DJ, Davis TN. 2006. Mps1 phosphorylation of Dam1 couples kinetochores to microtubule plus ends at metaphase. *Curr Biol* **16**:1489–1501. doi:10.1016/j.cub.2006.06.063
Sikorski RS, Boeke JD. 1991. In vitro mutagenesis and plasmid shuffling: from cloned gene to mutant yeast. *Meth Enzymol* **194**:302–318.
Storchová Z, Becker JS, Talarek N, Kögelsberger S, Pellman D. 2011. Bub1, Sgo1, and Mps1 mediate a distinct pathway for chromosome biorientation in budding yeast. *Mol Biol Cell* **22**:1473–1485. doi:10.1091/mbc.E10-08-0673
Straight AF, Marshall WF, Sedat JW, Murray AW. 1997. Mitosis in living budding yeast: anaphase A but no metaphase plate. *Science* **277**:574–8.
Tanaka T, Fuchs J, Loidl J, Nasmyth K. 2000. Cohesin ensures bipolar attachment of microtubules to sister centromeres and resists their precocious separation [In Process Citation]. *Nat Cell Biol* **2**:492–9.
Tanaka TU, Rachidi N, Janke C, Pereira G, Galova M, Schiebel E, Stark MJ, Nasmyth K. 2002. Evidence that the Ipl1-Sli15 (Aurora kinase-INCENP) complex promotes chromosome bi-orientation by altering kinetochore-spindle pole connections. *Cell* **108**:317–29.

Tsukahara T, Tanno Y, Watanabe Y. 2010. Phosphorylation of the CPC by Cdk1 promotes chromosome bi-orientation. *Nature* **467**:719–723. doi:10.1038/nature09390

Vader G, Cruijsen CWA, van Harn T, Vromans MJM, Medema RH, Lens SMA. 2007. The Chromosomal Passenger Complex Controls Spindle Checkpoint Function Independent from Its Role in Correcting Microtubule–Kinetochore Interactions. *Mol Biol Cell* **18**:4553–4564. doi:10.1091/mbc.E07-04-0328

van der Waal MS, Saurin AT, Vromans MJM, Vleugel M, Wurzenberger C, Gerlich DW, Medema RH, Kops GJPL, Lens SMA. 2012. Mps1 promotes rapid centromere accumulation of Aurora B. *EMBO Rep* **13**:847–854. doi:10.1038/embor.2012.93

Vanoosthuyse V, Hardwick KG. 2009. A Novel Protein Phosphatase 1-Dependent Spindle Checkpoint Silencing Mechanism. *Curr Biol*. doi:10.1016/j.cub.2009.05.060

Vanoosthuyse V, Prykhozhij S, Hardwick KG. 2007. Shugoshin 2 Regulates Localization of the Chromosomal Passenger Proteins in Fission Yeast Mitosis. *Mol Biol Cell* **18**:1657–1669. doi:10.1091/mbc.E06-10-0890

Verzijlbergen KF, Nerusheva OO, Kelly D, Kerr A, Clift D, de Lima Alves F, Rappsilber J, Marston AL. 2014. Shugoshin biases chromosomes for biorientation through condensin recruitment to the pericentromere. *eLife* **3**. doi:10.7554/eLife.01374

Wang X, Yu H, Xu L, Zhu T, Zheng F, Fu C, Wang Z, Dou Z. 2014. Dynamic autophosphorylation of mps1 kinase is required for faithful mitotic progression. *PLoS ONE* **9**:e104723. doi:10.1371/journal.pone.0104723

Weiss E, Winey M. 1996. The Saccharomyces cerevisiae spindle pole body duplication gene MPS1 is part of a mitotic checkpoint. *J Cell Biol* **132**:111–23.

Wu X, Tatchell K. 2001. Mutations in Yeast Protein Phosphatase Type 1 that Affect Targeting Subunit Binding †. *Biochemistry* **40**:7410–7420. doi:10.1021/bi002796k

Yamagishi Y, Yang C-H, Tanno Y, Watanabe Y. 2012. MPS1/Mph1 phosphorylates the kinetochore protein KNL1/Spc7 to recruit SAC components. *Nat Cell Biol* **14**:746–752. doi:10.1038/ncb2515

Zhang G, Kruse T, López-Méndez B, Sylvestersen KB, Garvanska DH, Schopper S, Nielsen ML, Nilsson J. 2017. Bub1 positions Mad1 close to KNL1 MELT repeats to promote checkpoint signalling. *Nature Communications* **8**:15822. doi:10.1038/ncomms15822

Zhu T, Dou Z, Qin B, Jin C, Wang X, Xu L, Wang Zhaoyang, Zhu L, Liu F, Gao X, Ke Y, Wang Zhiyong, Aikhionbare F, Fu C, Ding X, Yao X. 2013. Phosphorylation of microtubule-binding protein Hec1 by mitotic kinase Aurora B specifies spindle checkpoint kinase Mps1 signaling at the kinetochore. *J Biol Chem* **288**:36149–36159. doi:10.1074/jbc.M113.507970

FIGURE LEGENDS

Figure 1. The *mps1-3* mutant is defective in chromosome biorientation.

A: Serial dilutions of stationary phase cultures of the indicated strains were spotted on YEPD and incubated at the indicated temperatures. **B:** Mps1 sequence alignment around *S. cerevisiae* Ser635. Sc: *Saccharomyces cerevisiae*; Sp: *Schizosaccharomyces pombe*; Mm: *Mus musculus*: Hs: *Homo sapiens*; Dm: *Drosophila melanogaster*. **C-D:** Wild type, *mps1-3* and *mps1-1* mutant cells were synchronised in G1 with α-factor at permissive temperature (25°C) and then released at restrictive temperature (34°C, t=0). Cells were collected at the indicated time points for FACS analysis of DNA contents (**C**) and for immunofluorescence using anti-tubulin antibodies in order to score metaphase and anaphase spindles (**D**). Budding and nuclear division were scored on the FACS samples. **E:** Frequencies of chromosome loss were quantified at permissive temperature (25°C). **F:** Wild type and *mps1* mutant cells bearing the TetO/TetR-GFP system to mark the centromere of chromosome V (Tanaka et al., 2000) and expressing the SPBs marker Spc97-mCherry were synchronised as in (**B-C**) and arrested in anaphase through the temperature-sensitive *cdc15-2* allele. At 120 and 150 minutes, cells were fixed for scoring chromosome V segregation (n≥172). Arrowheads indicate the sister chromatids of chromosome V. Error bars: SD. N=3. Representative images of cells for each genotype are shown on the right. Scale bar: 5 μm. **G:** Wild type and *mps1-3* mutant cells carrying the TetO/TetR-GFP markers for *CEN5* labelling and expressing mCherry-Tub1 were grown at 25°C and then shifted to 34°C for 1 hour before filming. Cells were filmed at 34°C every 2 minutes by time lapse fluorescence microscopy. DIC: differential interference contrast. Scale bar: 5 μm.

Figure 2. The *mps1-3* mutant is defective in SAC signalling and does not localise Mps1 at kinetochores.

A: Wild type and *mps1* mutant cells were synchronised in G1 with α-factor at 25°C and then released at 34°C in the presence of nocodazole (t=0). Cells were collected at the indicated time points for FACS analysis of DNA contents. **B:** Cells were treated as in (**A**) and after 2 hours from the release α-factor was re-added to prevent cells from undergoing a second cell cycle. Cell samples were collected at the indicated time points for western blot analysis of the indicated proteins. Pgk1 was used as loading control. Cyc: cycling cells. **C:** Top: *in vitro* kinase assays with recombinant Mps1 and Mps1-3 purified from *E. coli* and incubated at 34°C for the indicated times in the presence of radioactive ATP and a recombinant Spc105 N-terminal fragment (aa 1-320) as substrate. Bottom left: kinase activity was quantified on the autoradiographs by Image J and normalized to the levels of the full length protein on the Coomassie Blue-stained gel (right). Bottom right: 1µg of the recombinant Mps1 kinases used for kinase assays was loaded on SDS page and stained with Coomassie Blue for normalisation of kinase assays. **D:** Wild type and *mps1-3* cells were synchronised in G1 with α-factor at 25°C and then released at 34°C in the presence of nocodazole. Cells were collected after 90 minutes and fixed with formaldehyde for ChIP-seq analysis. ChIP sequence reads were normalised against sequence reads from corresponding input samples, and relative enrichment is plotted for chromosome III around the centromere (see the centromeric regions of all 16 yeast chromosomes in Fig. S2). *Y*-axis shows enrichment values (linear scale, range is 0–10). Values below 1.5 are shown in grey, and values above 1.5 (i.e. sequences enriched in ChIP samples) are red coloured. **E:** Cells with the indicated genotypes were synchronised in G1 with α-factor at 25°C and then released in fresh medium at 34°C (t=0). Cells were collected at the indicated time points for FACS analysis of DNA contents.

Figure 3. Characterisation of the extragenic suppressors of *mps1-3* mutant cells.

A: Serial dilutions of stationary phase cultures of the indicated strains were spotted on YEPD and incubated at 25°C and 34°C. **B:** List of extragenic suppressors found in the unbiased genetic screen. **C:** Serial dilutions of stationary phase cultures of the indicated strains were spotted on YEPD and incubated at the indicated temperatures. **D:** Cells with the indicated genotypes were synchronised in G1 with α-factor at 25°C and then released in fresh medium at 34°C in presence of nocodazole (t=0). Cells were collected at the indicated time points for FACS analysis of DNA contents. **E:** Cells were treated as in (**C**) and collected at the indicated time points for western blot analysis of Mad1-3HA. Cyc: cycling cells. **F:** Cells with the indicated genotypes were synchronised at 25°C and then released in fresh medium at 34°C (t=0). Cells were collected at the indicated time points for FACS analysis of DNA contents. **G-H:** Cells with the indicated genotypes carrying the TetO/TetR-GFP markers for *CEN5* labelling and expressing mCherry-Tub1 were grown at 25°C and then shifted to 34°C for one hour before filming. Cells were filmed at 34°C every 2 or 4 minutes by time lapse fluorescence microscopy. Chromosome V segregation errors are reported in the table (**H**). Representative cells are shown as examples in the montages (**G**). Representative montages for wild type and *mps1-3* cells are shown in Fig. 1F. DIC: differential interference contrast. Scale bar: 5 µm. **I:** Wild type, *mps1-3, mps1-3 spc105-18,* and *mps1-3 GLC7-24* cells were synchronised in G1 with α-factor at 25°C and then released at 32°C in the presence of nocodazole (note that the presence of 3HA tags at the C-terminus of Mps1-3 slightly decreases the maximal temperature of suppression). Cells were collected after 90 minutes and fixed with formaldehyde for ChIP-seq analysis. ChIP sequence reads were normalised against sequence reads from corresponding input samples, and relative enrichment is plotted for chromosome III around the centromere (see the centromeric regions of all 16 yeast chromosomes in Fig. S5). *Y*-axis shows enrichment values (linear scale, range is 0–10).

Values below 1.5 are shown in grey, and values above 1.5 (i.e. sequences enriched in ChIP samples) are red coloured.

Figure 4. Spc105 phosphorylation and Bub1 kinetochore recruitment are impaired in *mps1-3* cells.

A-B: Wild type and *mps1-3* cells were synchronised in G1 with α-factor at 25°C and then released at 34°C in the presence (**A**) or absence (**B**) of nocodazole (t=0). Cells were collected at the indicated time points for western blot analysis of the indicated proteins. Equal amounts of protein extracts were loaded on two different gels, for western blot of Spc105-3PK and Clb2/Pgk1 respectively. Clb2 was used as mitotic marker and Pgk1 as loading control. Cyc: cycling cells. **C-D:** Cells with the indicated genotypes expressing Bub1-GFP and the kinetochore marker Mtw1-Tomato were grown in SD glu 2% and then shifted to 34°C for 1 hour before filming; they were then filmed every 4 minutes by time lapse fluorescence microscopy at 34°C. Note that *BUB1-GFP* is synthetic lethal with *mps1-3.* Thus, we used *mps1-3 GALs-MPS1 BUB1-GFP* cells that were grown in -His RG medium at 30°C; glucose was added to the culture for 30 minutes to shut off *GALs-MPS1*, followed by shifting cells to SD medium at 34°C for 1 before imaging in the same medium. Montages show representative cells (**C**). Arrowheads indicate Bub1-GFP signals at kinetochores. DIC: differential interference contrast. Scale bar: 5 μm. GFP signals (Bub1) co-localizing with Tomato signals (kinetochores) were scored on the movies (**D). E-H:** Wild type and *mps1-3* cells were synchronised in G1 with α-factor at 25°C and then released at 34°C in the presence (**E-F**) or absence (**G-H**) of nocodazole (t=0). Cells were collected at the indicated time points for western blot analysis of the indicated proteins **(E, G)** and for FACS analysis of DNA contents **(F, H)**. Equal amounts of protein extracts were loaded on two different gels, for western blot of Bub1-3HA/Cdc5 and Clb2/Pgk1 respectively. A white asterisk indicates a phosphorylated

isoform of Bub1 that in wild type cells correlates with lack of chromosome biorientation. Cdc5 and Clb2 were used as mitotic marker and Pgk1 as loading control. Cyc: cycling cells.

Figure 5. Artificial recruitment of Bub1 to Spc105 is sufficient to suppress the chromosome biorientation defects of *mps1-3* cells.

A: *SPC105-GBD* cells expressing Bub1-GFP were grown at 30°C and filmed every 4 minutes at 30°C by time lapse fluorescence microscopy. DIC: differential interference contrast. Scale bar: 5 μm. **B:** Serial dilutions of stationary phase cultures of the indicated strains were spotted on YEPD and incubated at the indicated temperatures. **C:** cells with the indicated genotypes were grown at 25°C and then shifted at 34°C (t=0). Every hour after the temperature shift the same number of cells was plated on YEPD for each strain and incubated at 25°C to determine the number of colony-forming units. Percentages of viable cells have been calculated for each strain relative to t=0. Error bars: SD. N=3. **D:** Cells with the indicated genotypes were synchronised in G1 with α-factor at 25°C and then released in fresh medium at 34°C. Cells were collected at the indicated time points for FACS analysis of DNA contents.

SUPPLEMENTAL MATERIAL

Figure S1. The *mps1-3* mutant proficiently assembles and elongates bipolar spindles and does not undergo premature chromatid separation.

A: Wild type and *mps1* mutant cells expressing Tub1-GFP have been filmed by time-lapse video-microscopy every 4 minutes at 34°C. DIC: differential interference contrast. Scale bar: 5 µm. **B:** Wild type and *mps1* mutant cells carrying the tetO/tetR-GFP system to label the arms of chromosome V (Michaelis et al., 1997) and the *cdc16-1* temperature-sensitive allele were synchronised with α-factor at 25°C and then released at t=0 at 37°C (restrictive temperature for both *mps1* mutant alleles and *cdc16-1*). At the indicated times, samples have been fixed in ethanol for scoring. Premature chromatid separation in metaphase was identified by two separated GFP dots of chromosome V, while one single dot represented unseparated chromatids. n≥200 N=3. Error bars: SD. **C:** *mps1* mutant cells carrying the tetO/tetR-GFP system to label *CEN5* and expressing mCherry-Tub1 were arrested in G1 with α-factor at 25°C and then released at 34°C for filming every 4' for 5 hours. Representative frames of cells in G1 (t=0) and in the first anaphase are shown. DIC: differential interference contrast. Scale bar: 5 µm.

Figure S2. The Mps1-3 has elevated kinase activity and increased protein levels *in vivo*.

A: Top: GST-tagged Mps1, Mps1-3 and Mps1-1 expressed from the *GAL1* promoter (Lauzé et al., 1995) were affinity purified and incubated *in vitro* with radioactive ATP and myelin basic protein (MBP) for the indicated times. Bottom left: 0.2, 0.1 and 0.05 OD_{280} of each extract were loaded on SDS page for western blot analysis with an anti-GST antibody to quantify Mps1 protein levels. Note that Mps1 overexpression from the *GAL1* promoter leads

to accumulation of Mps1 phosphorylated isoforms. Right: autophosphorylation and MBP kinase activity was quantified at each time point on the autoradiographs by Image J and normalized to the protein levels quantified by Image J in the lowest OD_{280} (0.05). A.U.: Arbitrary units. **B:** Cells expressing 3HA-tagged Mps1 (wild type) or Mps1-3 cells were grown at 25°C, synchronised in G1 with α-factor and released into the cell cycle at 34°C to monitor Mps1 protein levels at the indicated time points by western blot. α-factor was re-added after 60' to re-accumulate cells in the next G1 phase (note, however, that wild type cells re-entered into a new cell cycle at 135'). Clb2 was used as mitotic marker, while Pgk1 was used as loading control. Mps1 protein levels were quantified by ImageJ and normalised to Pgk1 levels. A.U.: Arbitrary units.

Figure S3. The Mps1-3 mutant protein fails to accumulate at kinetochores

Wild type and *mps1-3* cells were synchronised in G1 with α-factor at 25°C and then released at 34°C in the presence of nocodazole. Cells were collected after 90 minutes and fixed with formaldehyde for ChIP-seq analysis. ChIP sequence reads were normalised against sequence reads from corresponding input samples, and relative enrichment is plotted for all yeast chromosomes except for chromosome III (shown in Fig. 2D) around the centromere. *Y*-axis shows enrichment values (linear scale, range is 0–10). Values below 1.5 are shown in grey, and values above 1.5 (i.e. sequences enriched in ChIP samples) are red coloured.

Figure S4. The *GLC7-24* mutation might impair PP1 activity at kinetochores

A: Cells with the indicated genotypes were grown at 25°C in YEP containing 4% glucose (glu) and then shifted to YEP containing 1% glucose for 5 minutes. Cells were collected for western blot analysis in the two conditions. The phosphorylated active form of Snf1 was detected with anti-phospho AMPK (Thr172 that corresponds to Thr210 of Snf1), while an

anti-PK antibody was used to detect total levels of Snf1-3PK. Signals were quantified by ImageJ and the signals due to Snf1 phosphorylation were normalised for the total amounts of Snf1, in turn normalised for the amounts of Pgk1 in each lane (loading control). Error bars: SD. N=3. **B:** Wild type and *GLC7-24* cells were synchronised with α-factor at 25°C and then released in fresh medium containing nocodazole at the same temperature (t=0). Cells were collected at the indicated time points for western blot analysis. Anti-HA antibodies have been used to detect Sli15-3HA. Clb2 was used as mitotic marker. Cyc: cycling cells.

Figure S5. The Mps1-3 mutant protein fails to re-accumulate at kinetochores in the *spc105-18* and *GLC7-24* suppressors.

Cells with the indicated genotypes were synchronised in G1 with α-factor at 25°C and then released at 32°C in the presence of nocodazole (note that the presence of 3HA tags at the C-terminus of Mps1-3 decreased the maximal permissive temperature of the suppressors from 34°C to 32°C). Cells were collected after 90 minutes and fixed with formaldehyde for ChIP-seq analysis. ChIP sequence reads were normalised against sequence reads from corresponding input samples, and relative enrichment is plotted for all yeast chromosomes except for chromosome V (shown in Fig. 3I) around the centromere. *Y*-axis shows enrichment values (linear scale, range is 0–10). Values below 1.5 are shown in grey, and values above 1.5 (i.e. sequences enriched in ChIP samples) are red coloured.

Figure S6. Suppression of the chromosome segregation defects of *mps1-3* mutant cells seems unlinked to Bub1 phosphorylation.

A: *mps1-3 spc105-18* cells were synchronised at 25°C with α-factor and then released in fresh medium containing nocodazole at 34°C (t=0). Cells were collected at the indicated time points for western blot analysis of Spc105-3PK. Clb2 was used as mitotic marker and Pgk1 as

loading control. **B:** *mps1-3* cells expressing Bub1-GFP and the kinetochore marker Mtw1-Tomato were synchronised with α-factor at 25°C in SD medium and then released in fresh medium at the same temperature. After 40 minutes, cells have been collected for imaging by fluorescence microscopy. A representative cell is shown. Note that at permissive temperature Bub1 colocalizes with kinetochores. **C, D:** Cells with the indicated genotypes were synchronised at 25°C with α-factor and then released in fresh medium at 34°C in presence (**D**) or absence (**C**) of Nocodazole (t=0). At the indicated time points cells were withdrawn for western blot analysis of Bub1-3HA. Same amounts of protein extracts were loaded on two different gels to detect Bub1-3HA and Cdc5 separately from Clb2 and Pgk1. Cdc5 and Clb2 were used as mitotic markers, while Pgk1 as loading control.

Figure S7. Artificial recruitment of Bub1 to Spc105 is sufficient to suppress the chromosome biorientation and SAC defects of *mps1-3* cells.

A-B: Cells with the indicated genotypes were synchronised in G1 with α-factor at 25°C and then released in fresh medium at 34°C in the absence (**A**) and the presence (**B**) of nocodazole. Cells were collected at the indicated time points for FACS analysis of DNA contents.

Figure S8. The chromosome segregation defects of *mps1-3* cells are at least partially independent of Sgo1 and the CPC.

A: Wild type and *mps1-3* cells expressing Sgo1-GFP and Mtw1-Tomato were grown at 25°C in SD medium and then incubated at 34°C for one hour before filming. Cells were then filmed every 2 minutes by live cell imaging at 34°C. Arrowheads indicate Sgo1-GFP kinetochore signals. DIC: differential interference contrast. Scale bar: 5 μm. The table reports the percentage of cells for each strain with Sgo1 colocalizing with Mtw1 after deconvolution. **B:** Meiotic segregants were obtained by sporulation of diploid cells generated by crossing *mps1-*

3 and *sgo1Δ* haploid cells. **C:** Serial dilutions of stationary phase cultures of the indicated strains were spotted on YEPD and incubated at the indicated temperatures. **D:** Cells with the indicated genotypes were synchronised in G1 with α-factor at 25°C and then released in fresh medium at 34°C. Cells were collected at the indicated time points for FACS analysis of DNA contents. **E:** Cells with the indicated genotypes were synchronised at 25°C with α-factor and then released in fresh medium containing nocodazole at 34°C (t=0). At the indicated time points cells were withdrawn for western blot analysis of Dam1-3PK. Same amounts of protein extracts were loaded on two different gels to detect Dam1-3PK separately from Pgk1. Pgk1 was used as loading control.

Video S1. Constitutive recruitment of Bub1 to Spc105 does not affect cell cycle progression.

SPC105-GBD cells expressing Bub1-GFP were grown at 30°C and filmed every 4 minutes at 30°C by time lapse fluorescence microscopy. Scale bar: 5 μm.

FIGURE LEGENDS FOR REVIEWERS ONLY

Figure R1. Dam1 and Ndc80 are not critical Mps1 phosphorylation targets for chromosome bi-orientation.

A, B: Serial dilutions of stationary phase cultures of the indicated strains were spotted on YEPD and incubated at the indicated temperatures.

Figure R2. Mps1 electrophoretic mobility is affected in *mps1-3* mutants independently of the presence of suppressing mutations.

Cells with the indicated genotypes were synchronised at 25°C with α-factor and then released in fresh medium containing nocodazole at 34°C (t=0). At the indicated time points cells were withdrawn for western blot analysis of Mps1-3HA. Same amounts of protein extracts were loaded on two different gels to detect Mps1-3HA separately from Clb2 and Pgk1. Clb2 was used as mitotic marker; Pgk1 as loading control.

Figure R3. Phospho-mimicking mutations in the MELT repeats of Spc105 partially suppress the chromosome biorientation defects of *mps1-3* cells.

Cells with the indicated genotypes were synchronised in G1 with α-factor at 25°C and then released in fresh medium at 34°C in the absence (**A**) and the presence (**B**) of nocodazole. Cells were collected at the indicated time points for FACS analysis of DNA contents.

A

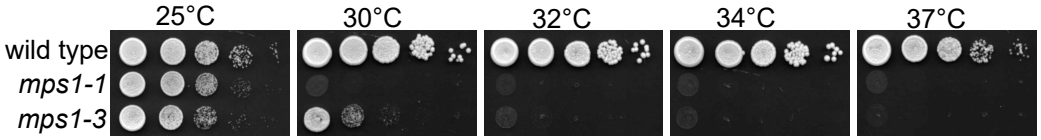

B

```
MPS1_Sc   EGNKWKVGRPSDMWSCGCIIY  647
MPH1L_Sp  GVKLVKLGRPSDVWSLGCILY  522
TTK_Mm    SKIRTKVSPRSDVWSLGCILY  726
TTK_Hs    GKSKSKISPKSDVWSLGCILY  727
MPS1_Dm   DQPKIKISTKSDVWSLGCILY  545
                  *:.  **:** ***:*
```

C

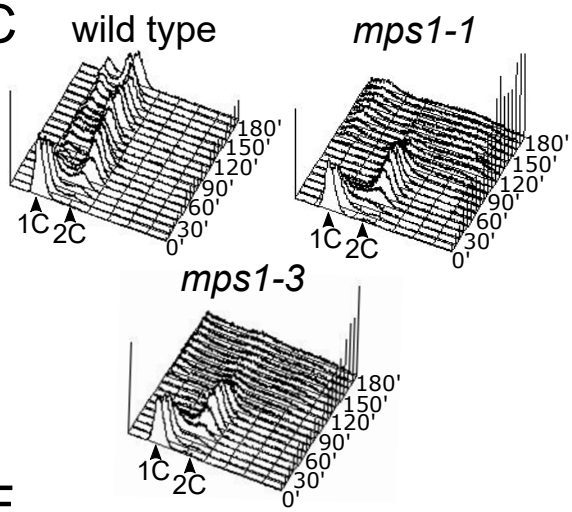

D

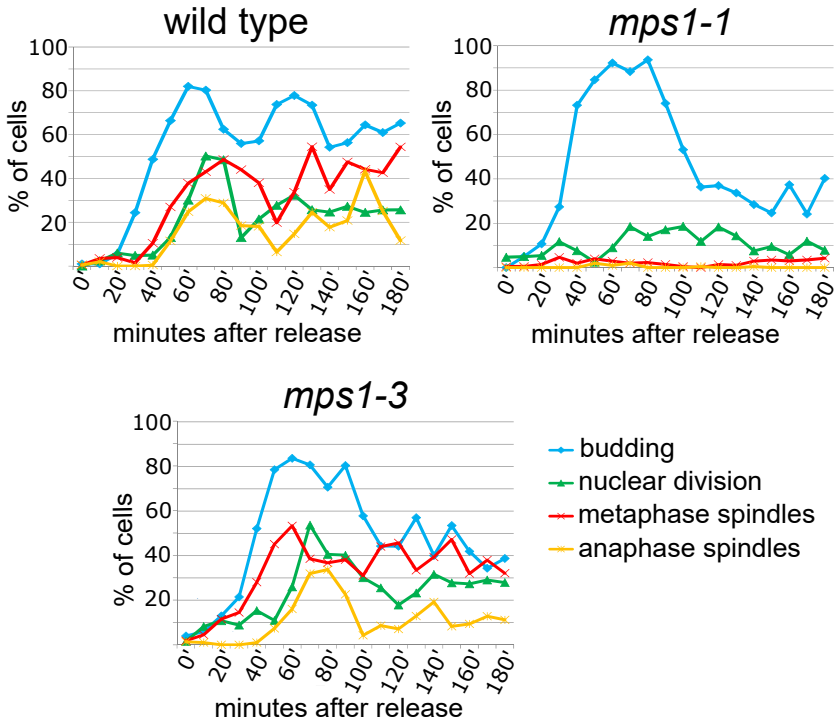

E

	Frequence of chromosome loss
wild type	1,7 x 10^{-8} for cell division
mps1-1	3,6 x 10^{-5} for cell division
mps1-3	1,82 x 10^{-5} for cell division

F

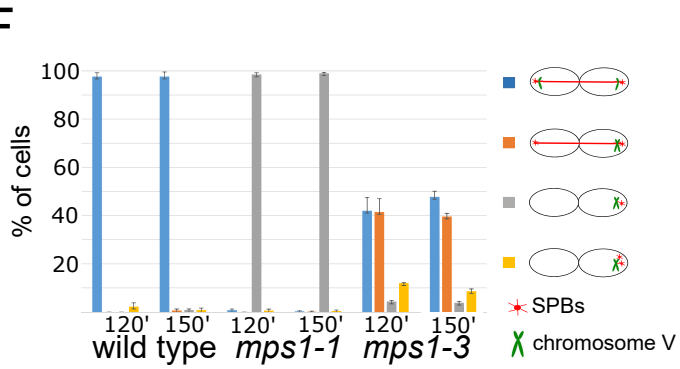

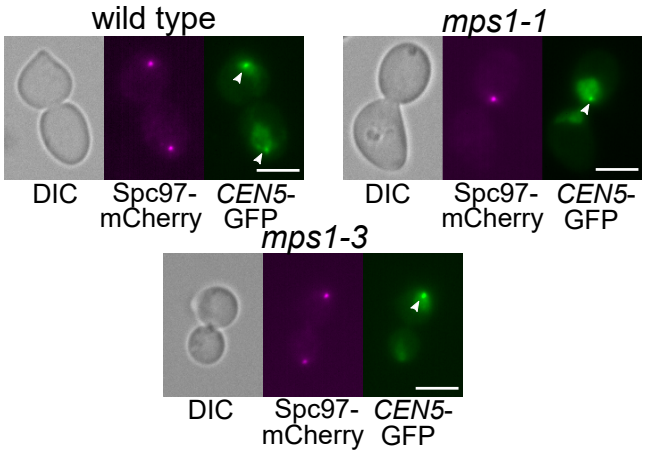

G

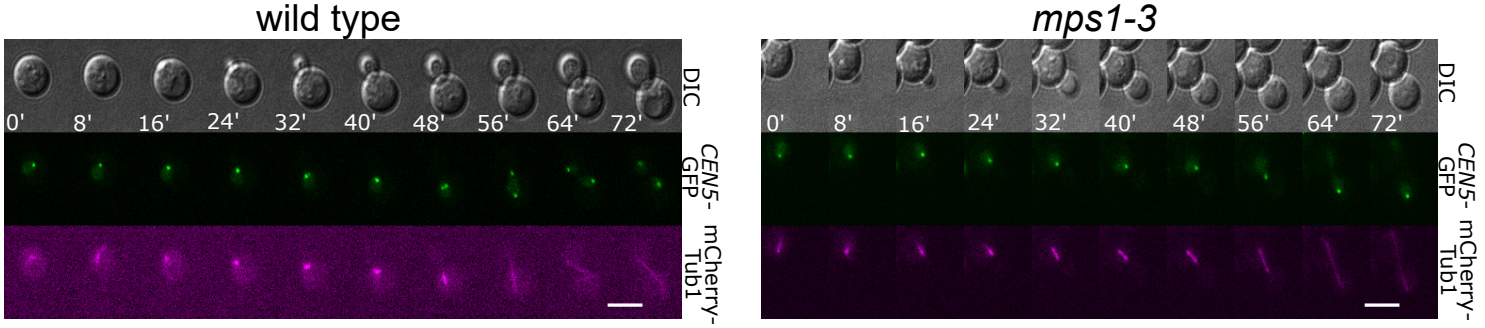

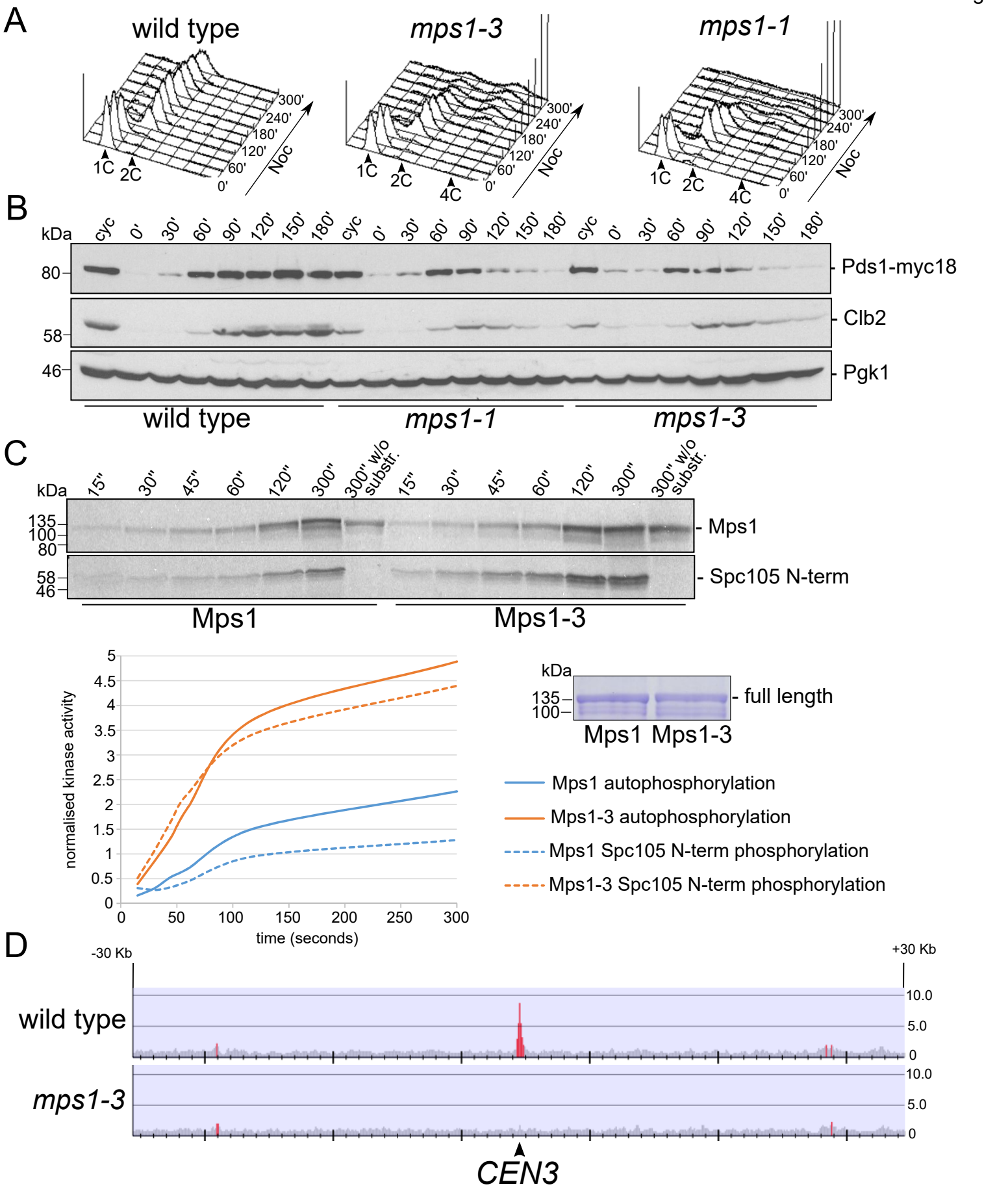
A
wild type
mps1-3
mps1-1
1C
2C
4C
Noc
0'
60'
120'
180'
240'
300'
B
kDa
cyc
0'
30'
60'
90'
120'
150'
180'
80
58
46
Pds1-myc18
Clb2
Pgk1
wild type
mps1-1
mps1-3
C
kDa
15"
30"
45"
60"
120"
300"
300" w/o substr.
135
100
80
58
46
Mps1
Spc105 N-term
Mps1
Mps1-3
normalised kinase activity
time (seconds)
full length
Mps1 autophosphorylation
Mps1-3 autophosphorylation
Mps1 Spc105 N-term phosphorylation
Mps1-3 Spc105 N-term phosphorylation
D
-30 Kb
+30 Kb
wild type
mps1-3
10.0
5.0
0
CEN3
E
wild type
mps1-3
MPS1-GFP mad2Δ MTW1-GBD
mps1-3-GFP mad2Δ MTW1-GBD
1C
2C
30'
60'
90'
120'
150'
180'

A

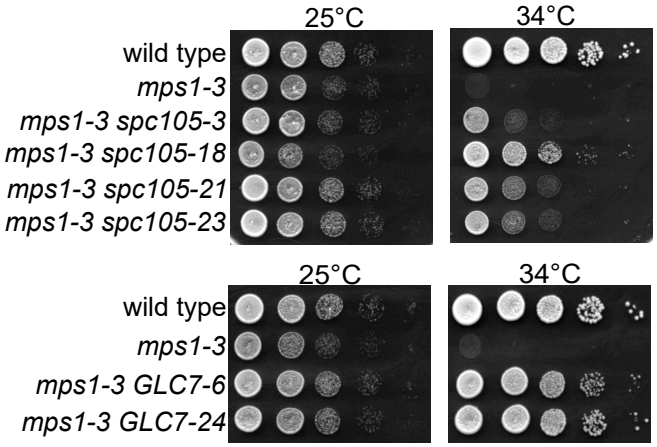

B

Suppressor	Gene	Aminoacid substitution
3	*SPC105*	Ala79Thr
18	*SPC105*	Val76Gly
21,23	*SPC105*	Val82Asp
6	*GLC7*	Phe256Ile
24	*GLC7*	Phe256Val
17	*GRR1* *RSC30*	Ser772Pro Gly571Asp
19	*GRR1* *RSC30*	Asn1069Lys Gly571Asp
20	*GRR1*	Ser772Pro
26	*GRR1* *RSC30*	Cys730Trp Gly571Asp

C

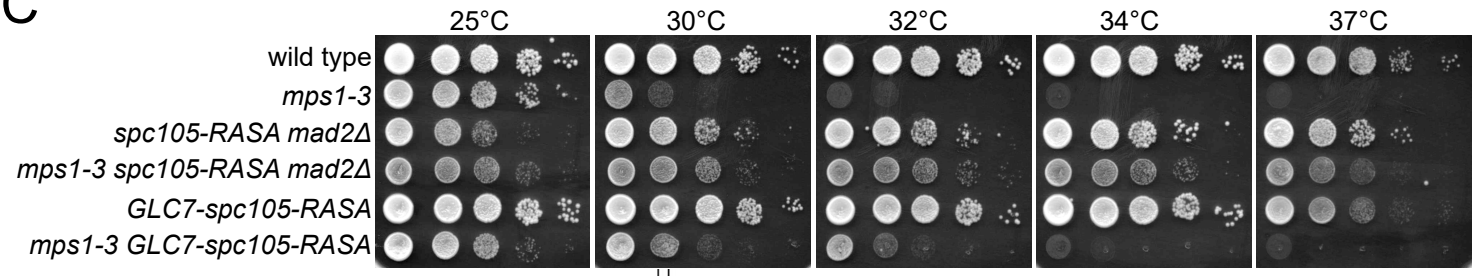

D

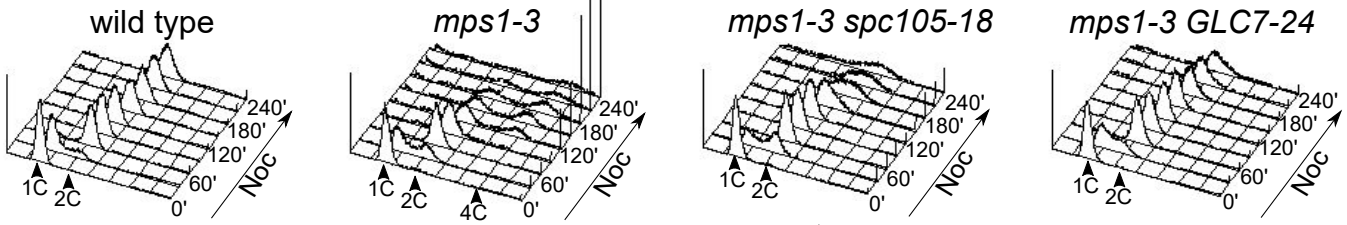

E

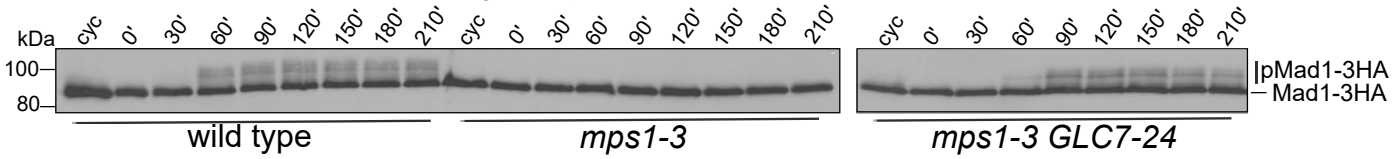

F

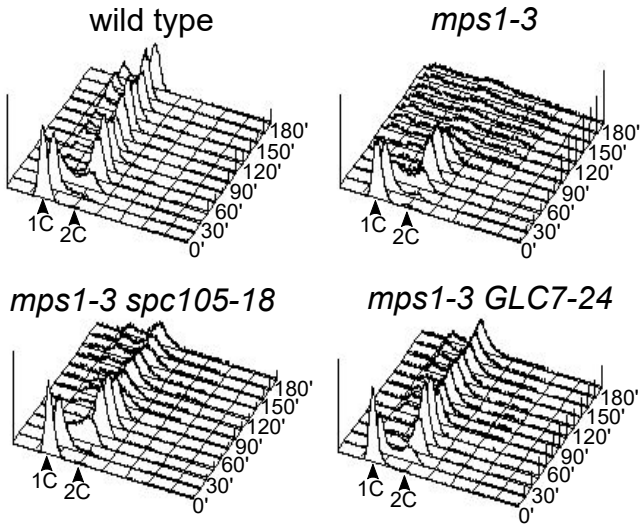

G

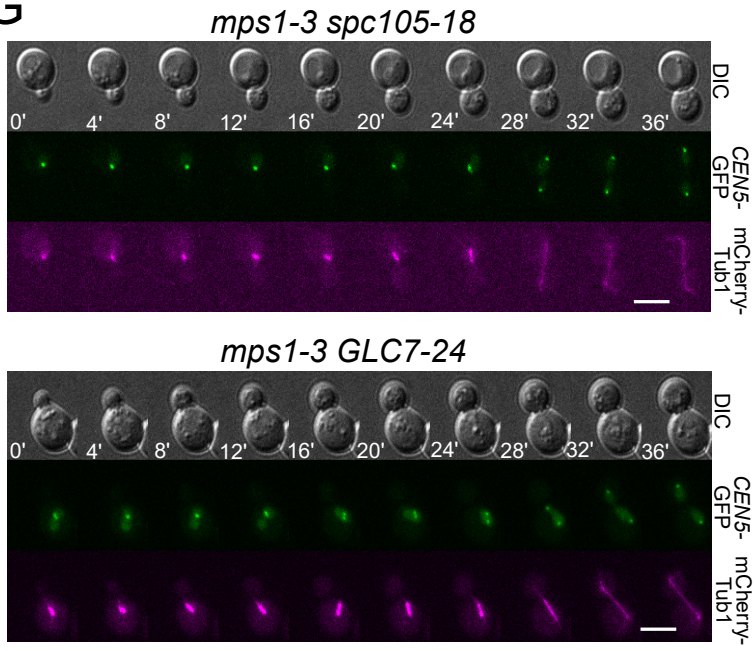

I

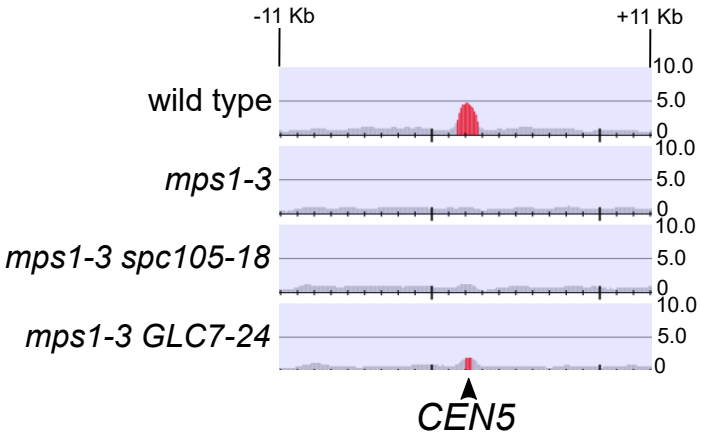

H

	normal segregation	missegregation		n
		mother	bud	
wild type	100%	/	/	201
mps1-3	51.3%	26.3%	22.4%	179
mps1-3 spc105-18	96.2%	0.3%	3.5%	341
mps1-3 GLC7-24	98.5%	0.4%	1.1%	272
mps1-3 spc105-18 mad2Δ	93.4%	3.5%	3.1%	198
mps1-3 GLC7-24 mad2Δ	92.7%	3.9%	3.5%	281

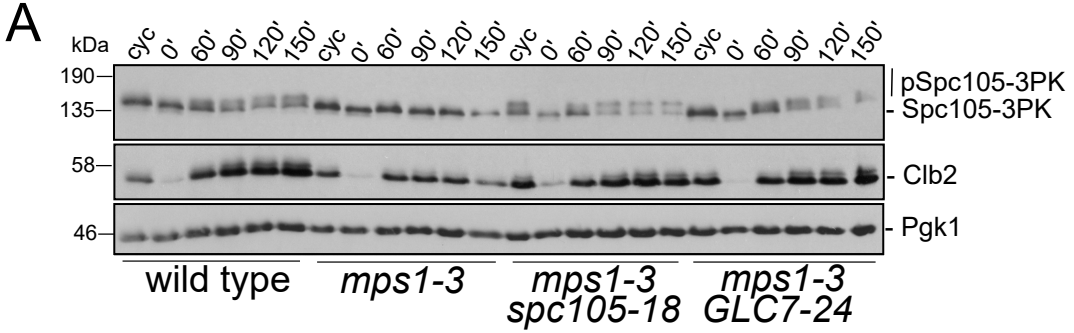

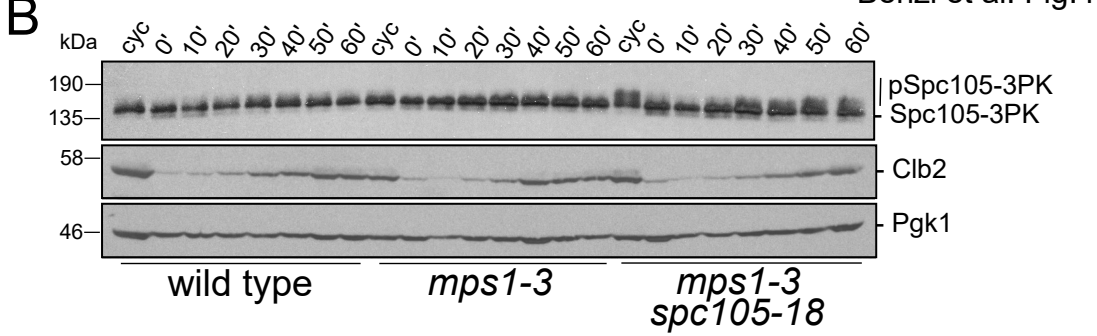

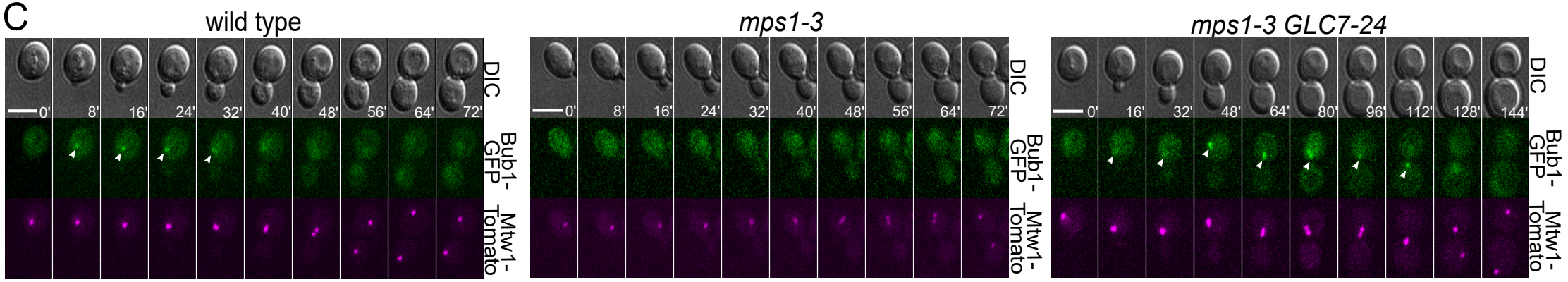

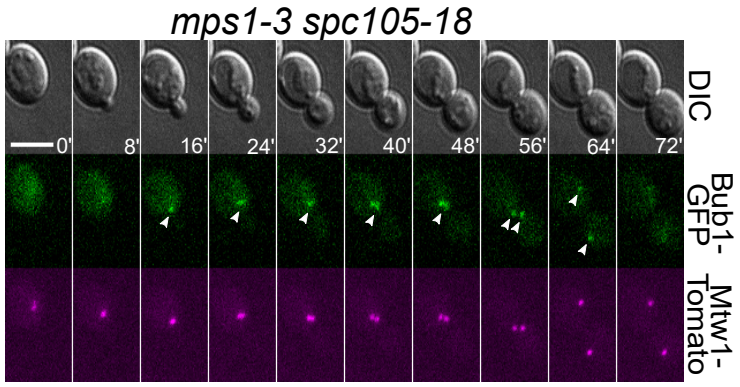

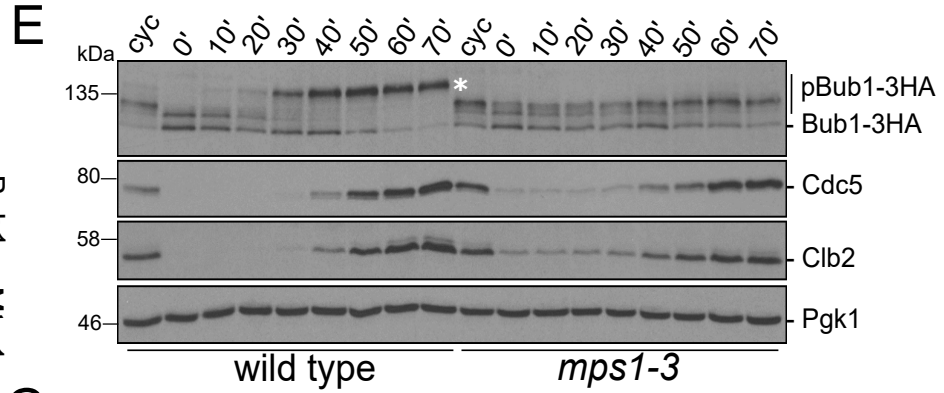

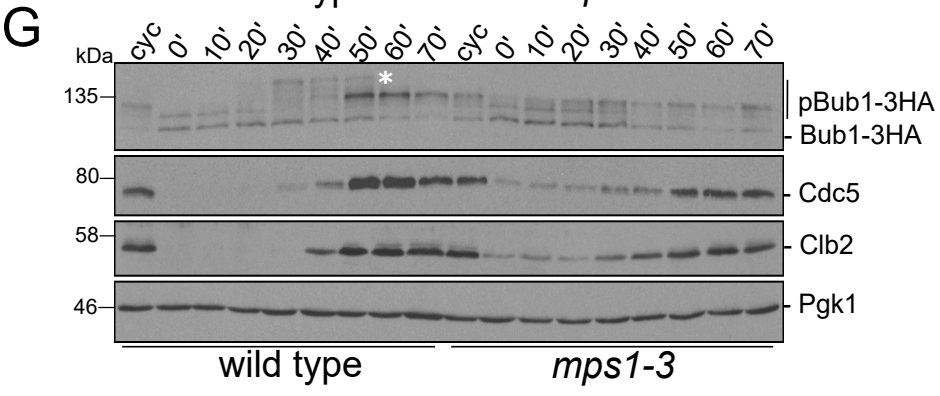

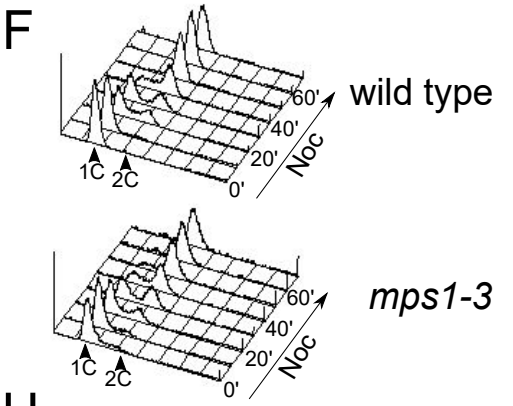

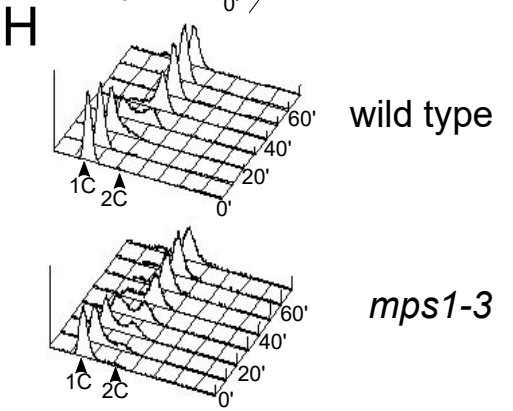

D

	Bub1 localization		n
	yes	no	
wild type	100%	/	260
mps1-3	20%	80%	170
mps1-3 spc105-18	95.7%	4.3%	214
mps1-3 GLC7-24	94.2%	5.8%	347

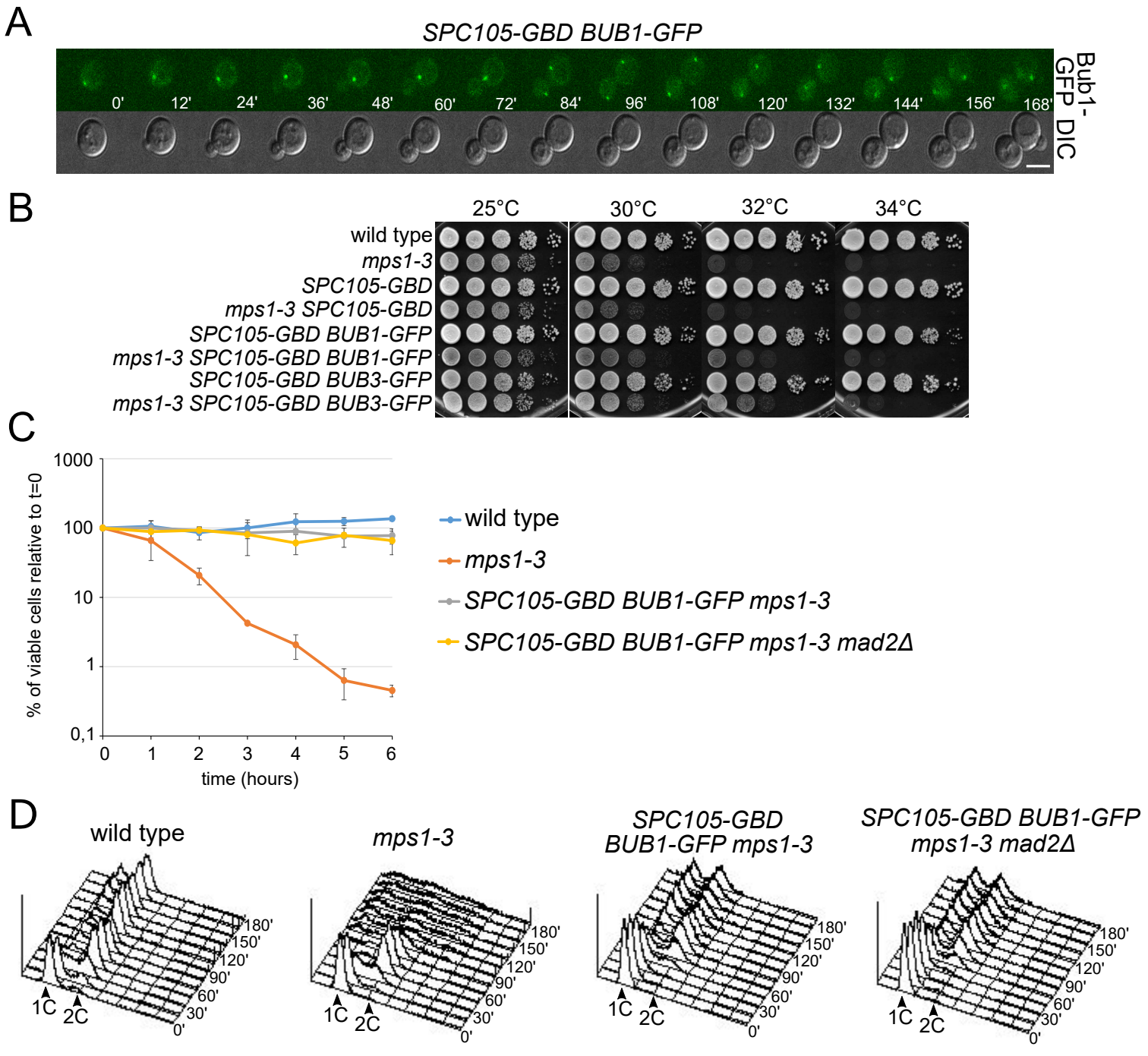
A
SPC105-GBD BUB1-GFP
0'
12'
24'
36'
48'
60'
72'
84'
96'
108'
120'
132'
144'
156'
168'
Bub1-GFP DIC
B
25°C
30°C
32°C
34°C
wild type
mps1-3
SPC105-GBD
mps1-3 SPC105-GBD
SPC105-GBD BUB1-GFP
mps1-3 SPC105-GBD BUB1-GFP
SPC105-GBD BUB3-GFP
mps1-3 SPC105-GBD BUB3-GFP
C
% of viable cells relative to t=0
1000
100
10
1
0,1
0
1
2
3
4
5
6
time (hours)
wild type
mps1-3
SPC105-GBD BUB1-GFP mps1-3
SPC105-GBD BUB1-GFP mps1-3 mad2Δ
D
wild type
mps1-3
SPC105-GBD BUB1-GFP mps1-3
SPC105-GBD BUB1-GFP mps1-3 mad2Δ
1C
2C
0'
30'
60'
90'
120'
150'
180'

A

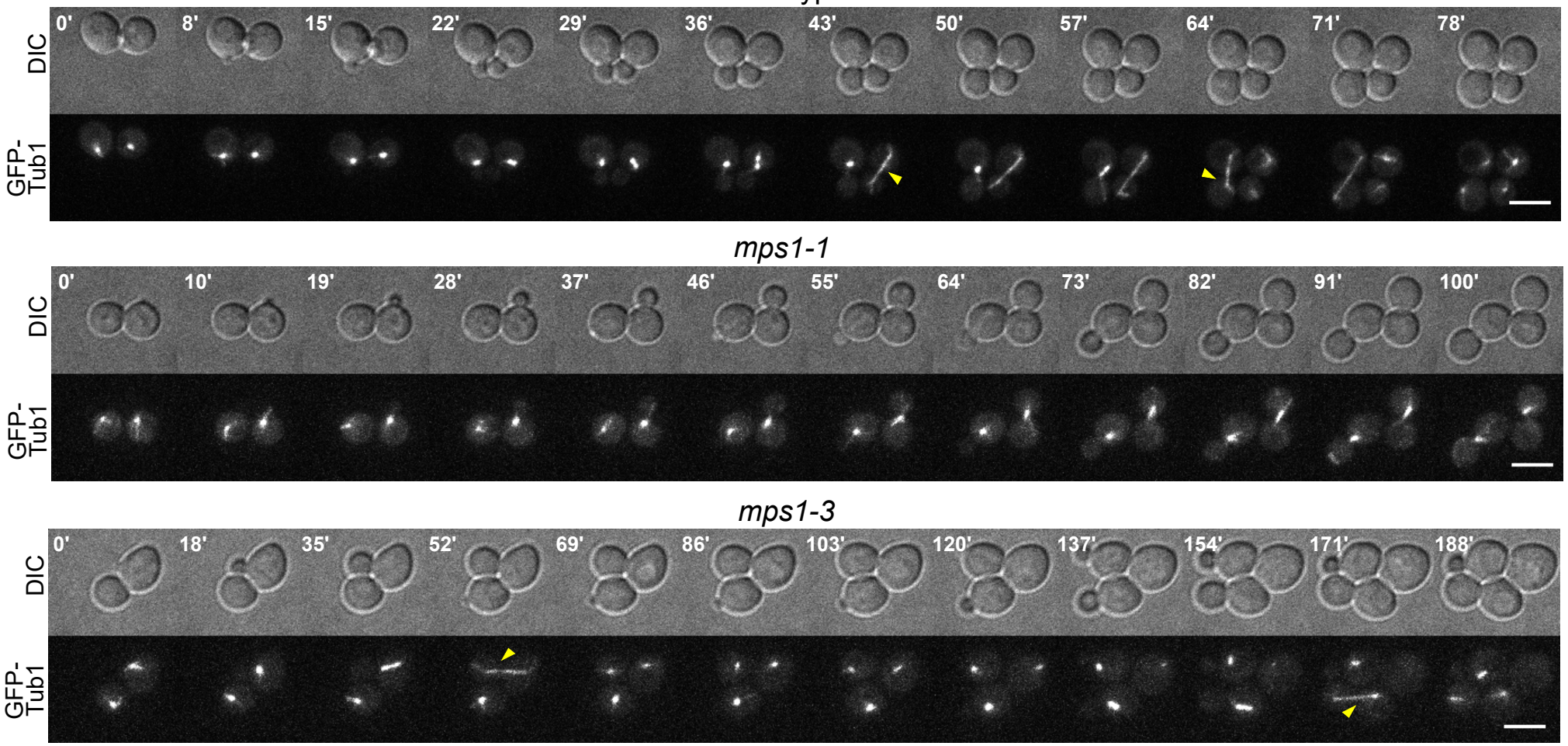

B

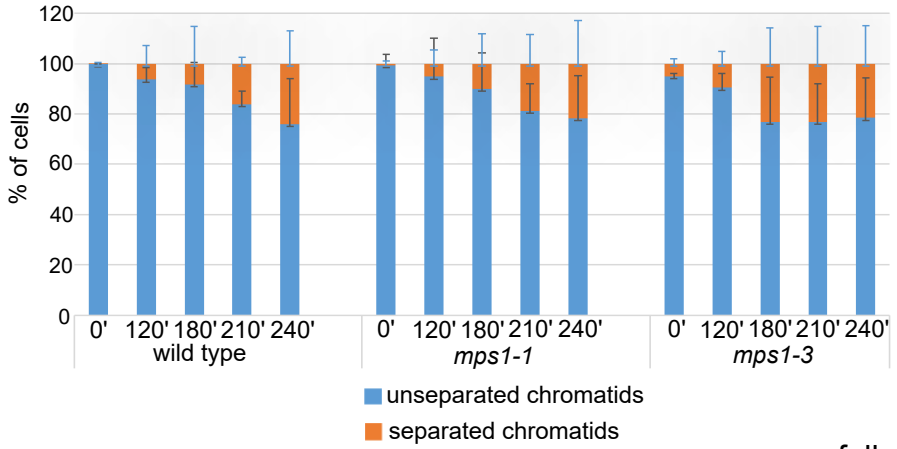

C

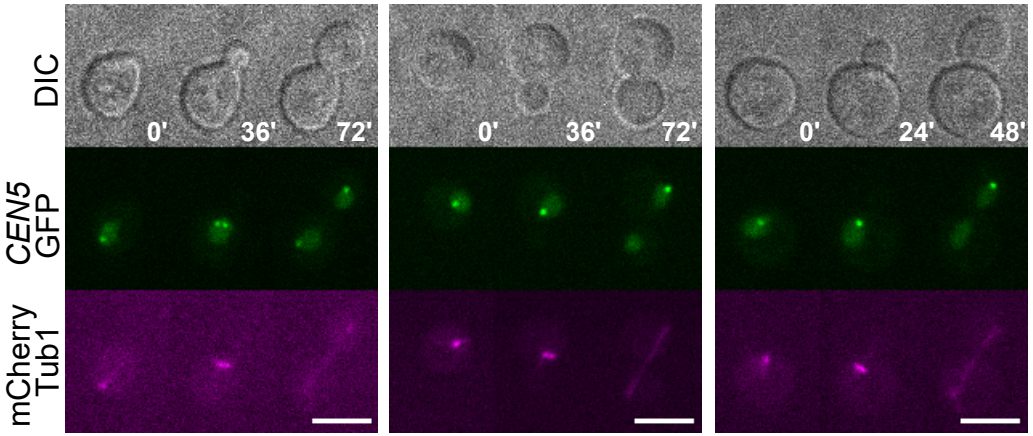

		mother	bud
first cycle	61.4% (n=51)	8.4% (n=7)	30.2% (n=25)
following cycles	59.5% (n=69)	18.1% (n=21)	22.4% (n=26)

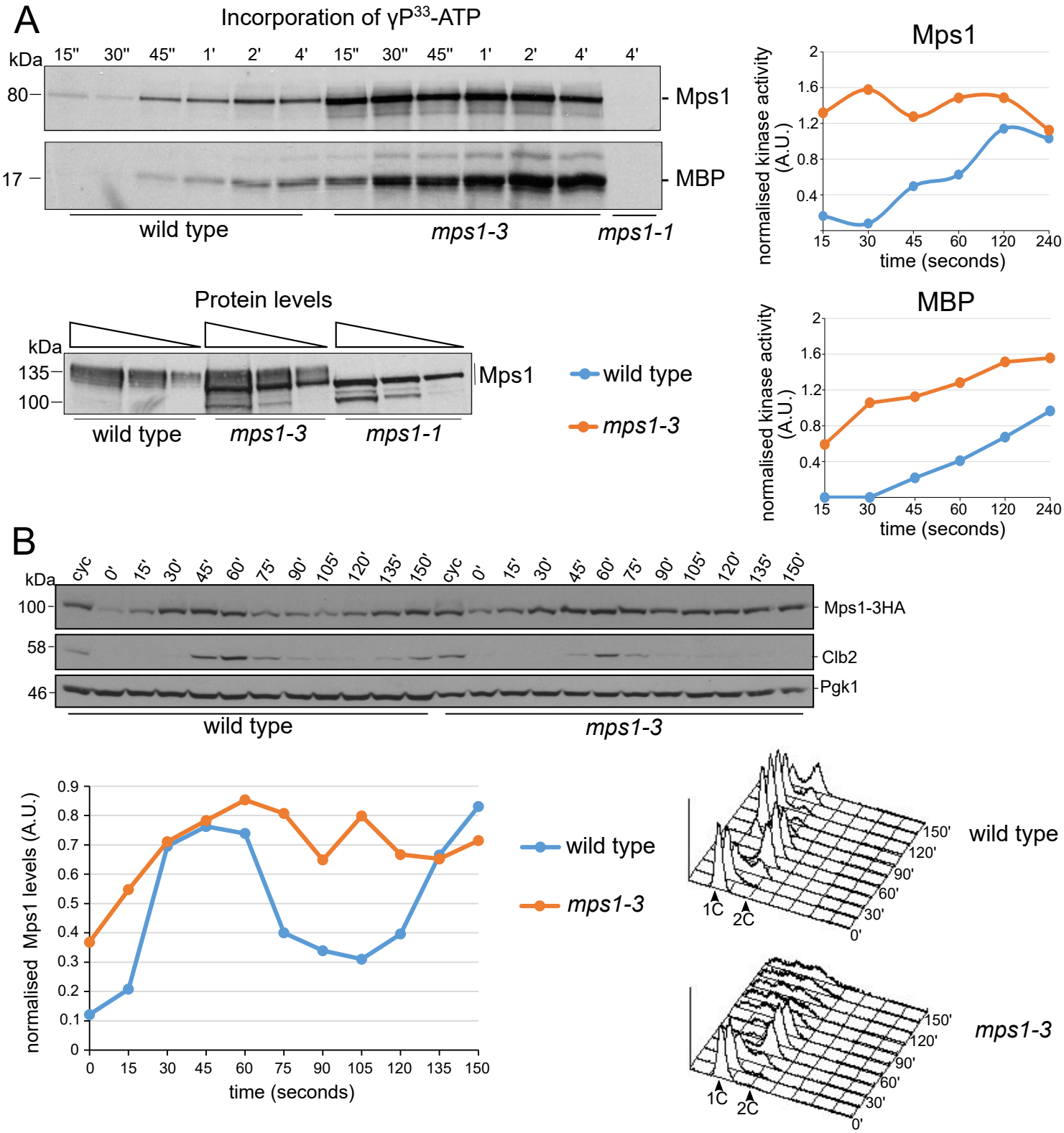
A
Incorporation of γP33-ATP
kDa
15" 30" 45" 1' 2' 4' 15" 30" 45" 1' 2' 4' 4'
80
Mps1
17
MBP
wild type
mps1-3
mps1-1
Protein levels
kDa
135
100
Mps1
wild type
mps1-3
mps1-1
wild type
mps1-3
Mps1
normalised kinase activity (A.U.)
time (seconds)
MBP
normalised kinase activity (A.U.)
time (seconds)
B
kDa
cyc 0' 15' 30' 45' 60' 75' 90' 105' 120' 135' 150' cyc 0' 15' 30' 45' 60' 75' 90' 105' 120' 135' 150'
100
Mps1-3HA
58
Clb2
46
Pgk1
wild type
mps1-3
normalised Mps1 levels (A.U.)
time (seconds)
wild type
mps1-3
1C
2C
150'
120'
90'
60'
30'
0'
wild type
mps1-3

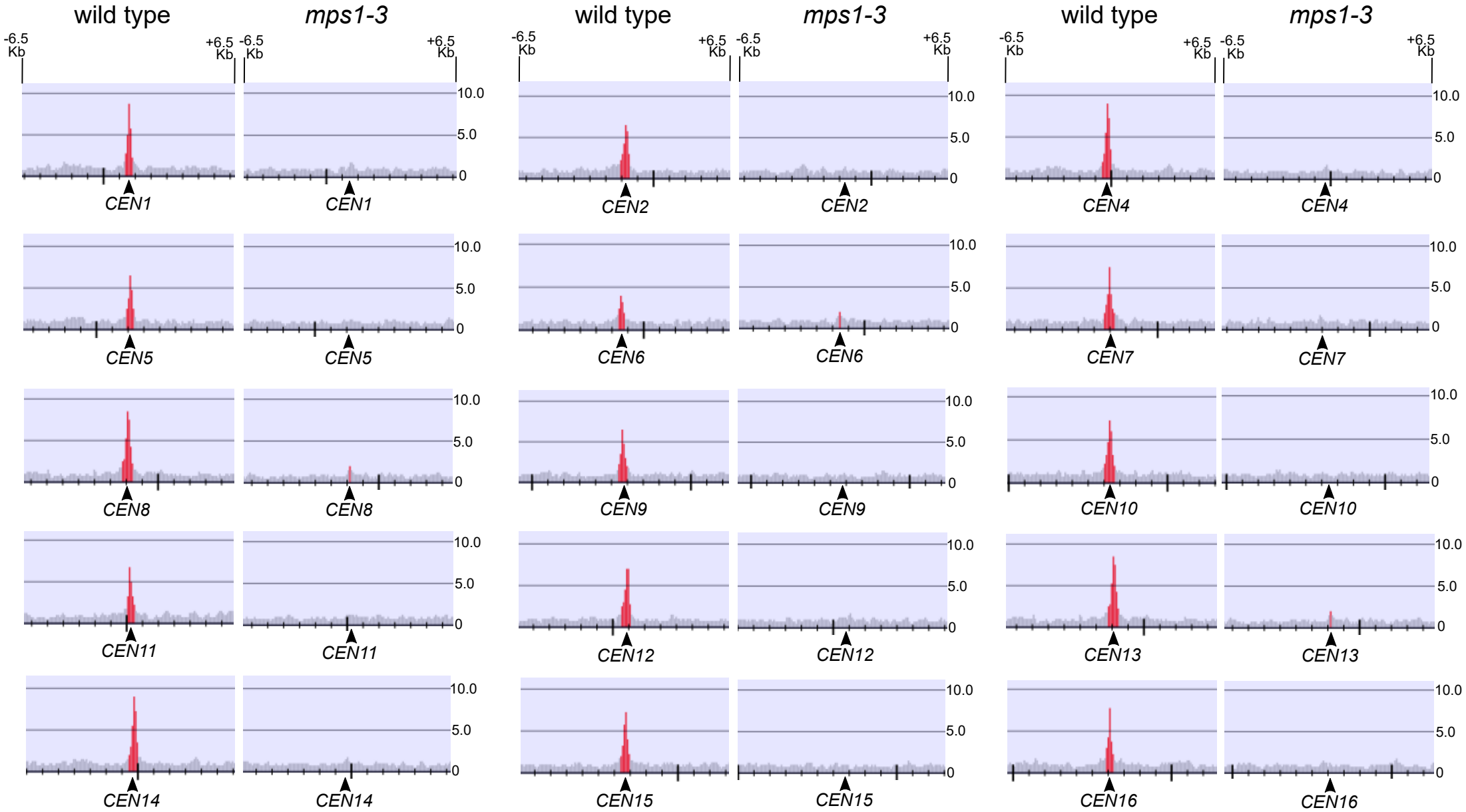
wild type
mps1-3
wild type
mps1-3
wild type
mps1-3
-6.5 Kb
+6.5 Kb
10.0
5.0
0
CEN1
CEN1
CEN2
CEN2
CEN4
CEN4
CEN5
CEN5
CEN6
CEN6
CEN7
CEN7
CEN8
CEN8
CEN9
CEN9
CEN10
CEN10
CEN11
CEN11
CEN12
CEN12
CEN13
CEN13
CEN14
CEN14
CEN15
CEN15
CEN16
CEN16

A

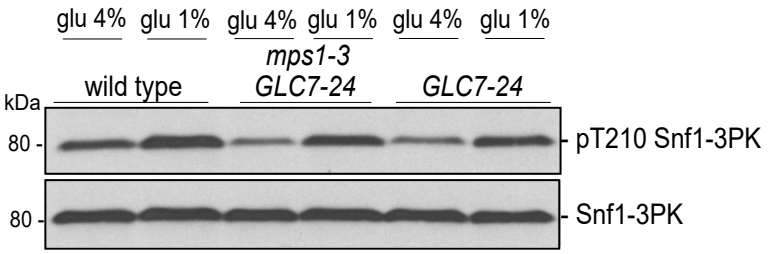
glu 4%
glu 1%
glu 4%
glu 1%
glu 4%
glu 1%
wild type
mps1-3
GLC7-24
GLC7-24
kDa
80
80
pT210 Snf1-3PK
Snf1-3PK

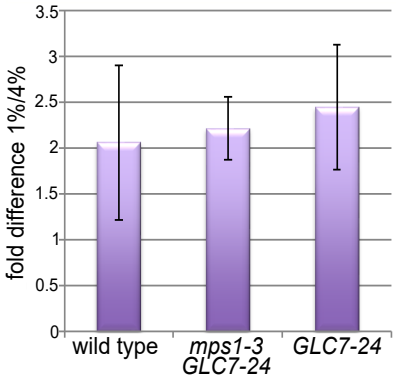
fold difference 1%/4%
3.5
3
2.5
2
1.5
1
0.5
0
wild type
mps1-3
GLC7-24
GLC7-24

B

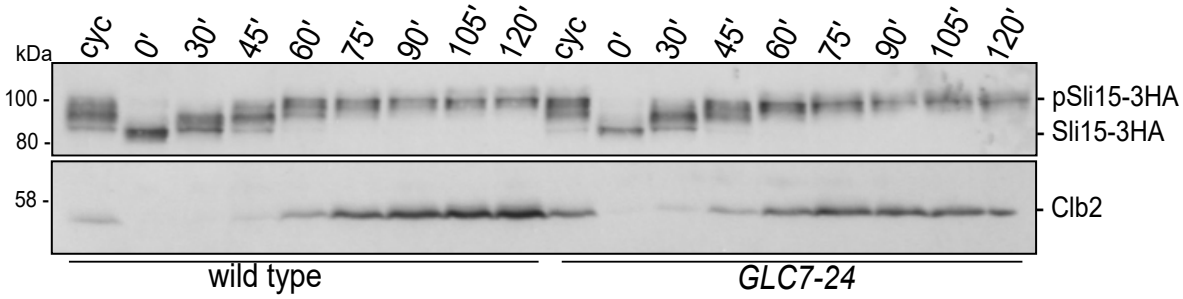
cyc
0'
30'
45'
60'
75'
90'
105'
120'
cyc
0'
30'
45'
60'
75'
90'
105'
120'
kDa
100
80
58
pSli15-3HA
Sli15-3HA
Clb2
wild type
GLC7-24

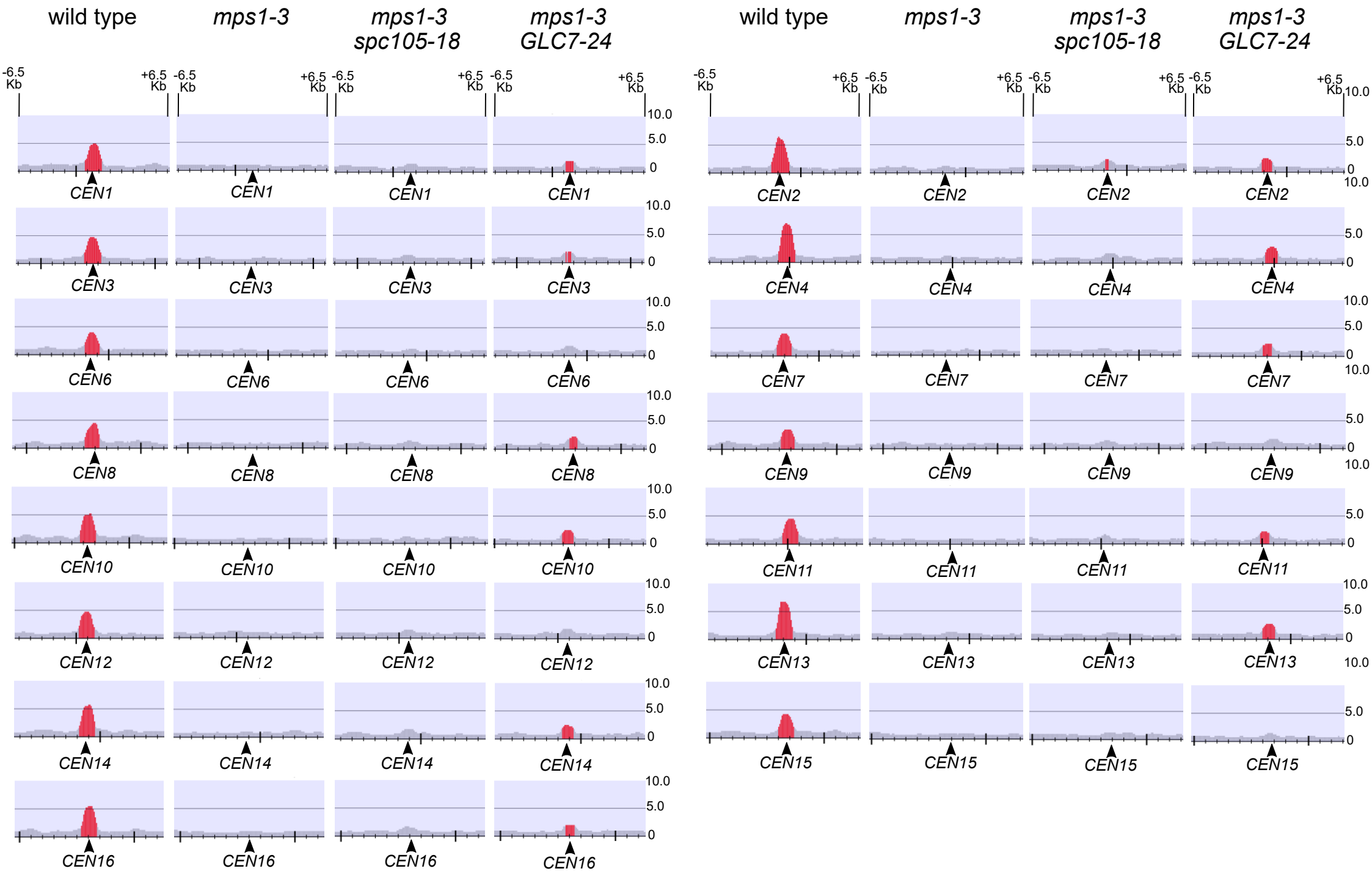
wild type
mps1-3
mps1-3 spc105-18
mps1-3 GLC7-24
wild type
mps1-3
mps1-3 spc105-18
mps1-3 GLC7-24
-6.5 Kb
+6.5 Kb
10.0
5.0
0
CEN1
CEN2
CEN3
CEN4
CEN6
CEN7
CEN8
CEN9
CEN10
CEN11
CEN12
CEN13
CEN14
CEN15
CEN16

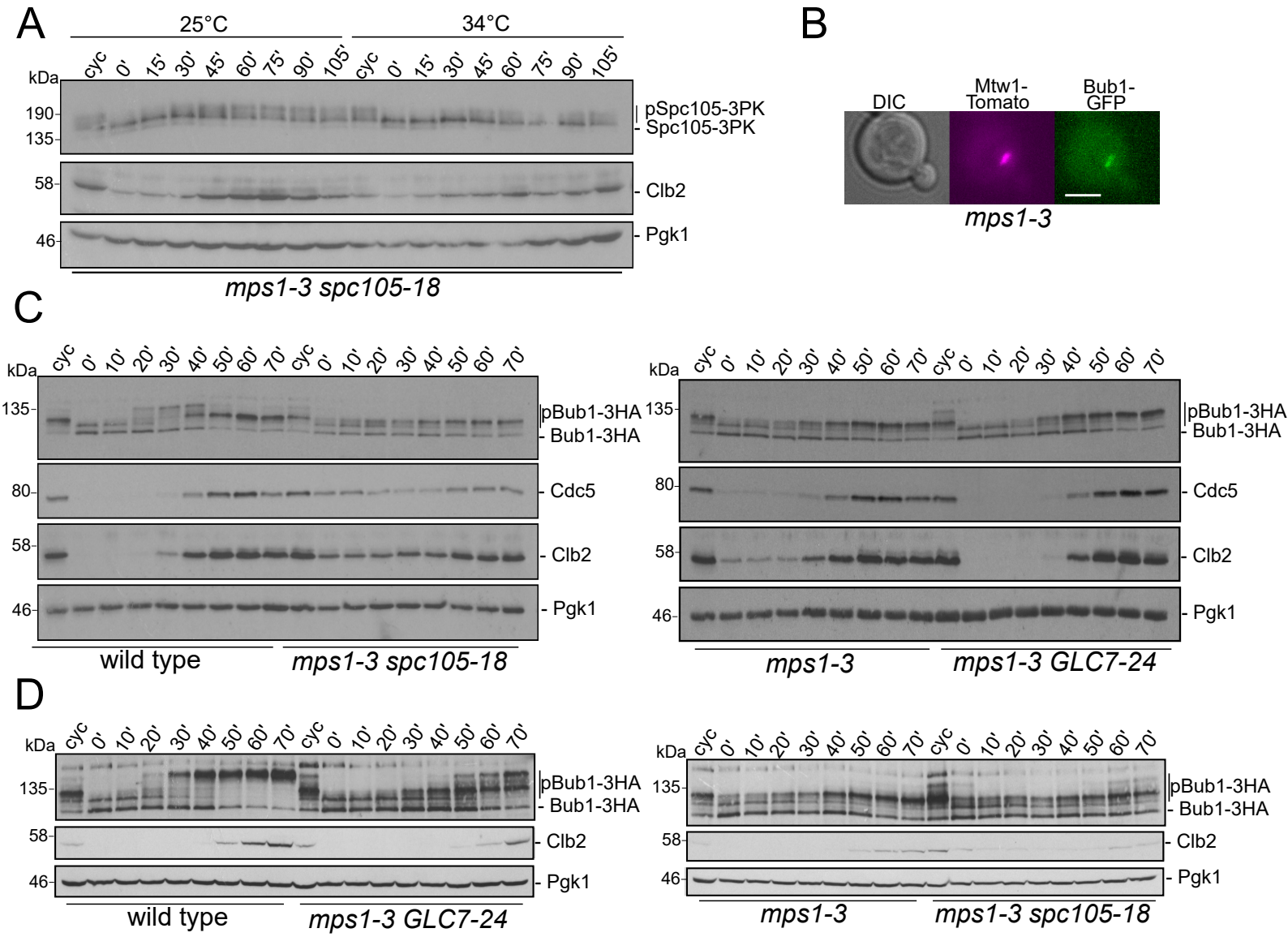
A
25°C
34°C
cyc 0' 15' 30' 45' 60' 75' 90' 105' cyc 0' 15' 30' 45' 60' 75' 90' 105'
kDa
190
135
58
46
pSpc105-3PK
Spc105-3PK
Clb2
Pgk1
mps1-3 spc105-18
B
DIC
Mtw1-Tomato
Bub1-GFP
mps1-3
C
cyc 0' 10' 20' 30' 40' 50' 60' 70' cyc 0' 10' 20' 30' 40' 50' 60' 70'
kDa
135
80
58
46
pBub1-3HA
Bub1-3HA
Cdc5
Clb2
Pgk1
wild type
mps1-3 spc105-18
mps1-3
mps1-3 GLC7-24
D
wild type
mps1-3 GLC7-24
mps1-3
mps1-3 spc105-18

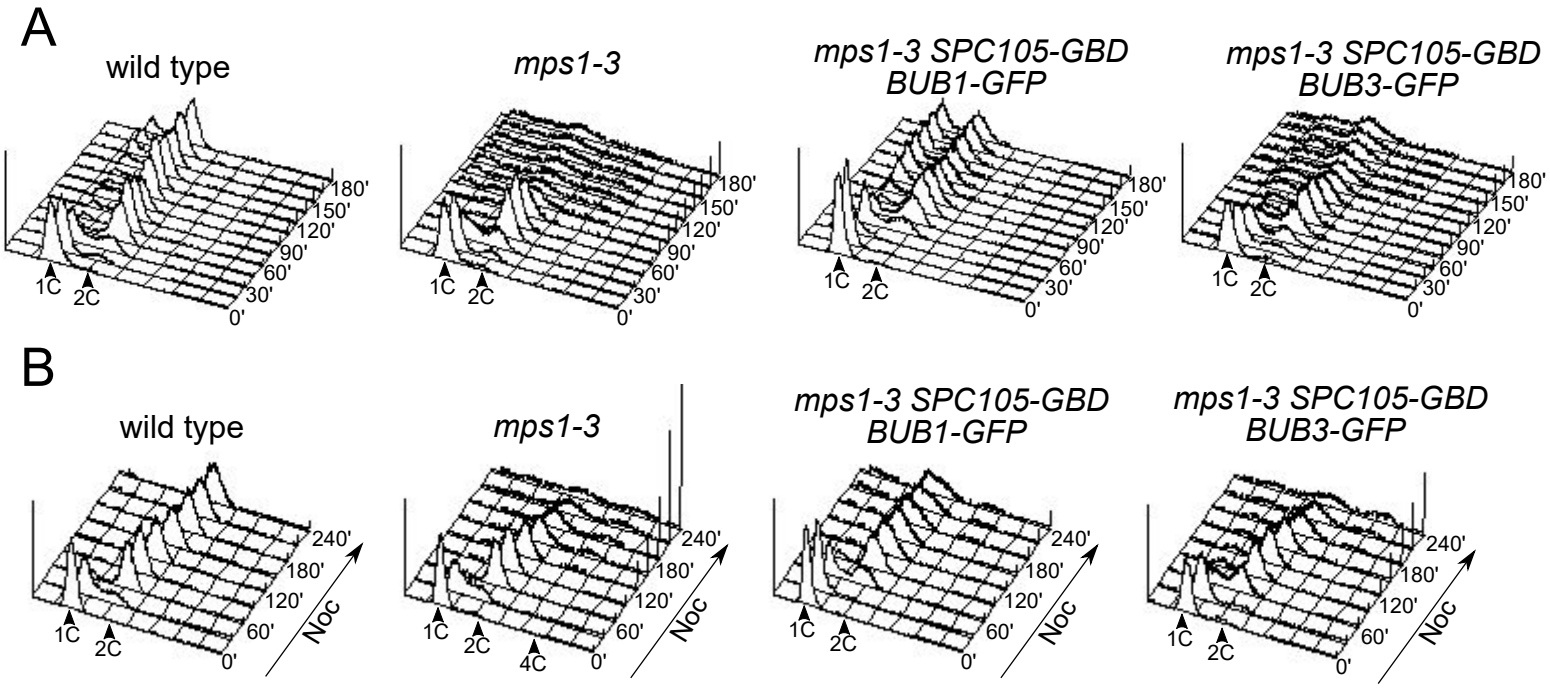
A
wild type
mps1-3
mps1-3 SPC105-GBD
BUB1-GFP
mps1-3 SPC105-GBD
BUB3-GFP
1C
2C
0'
30'
60'
90'
120'
150'
180'
B
wild type
mps1-3
mps1-3 SPC105-GBD
BUB1-GFP
mps1-3 SPC105-GBD
BUB3-GFP
1C
2C
4C
0'
60'
120'
180'
240'
Noc

A

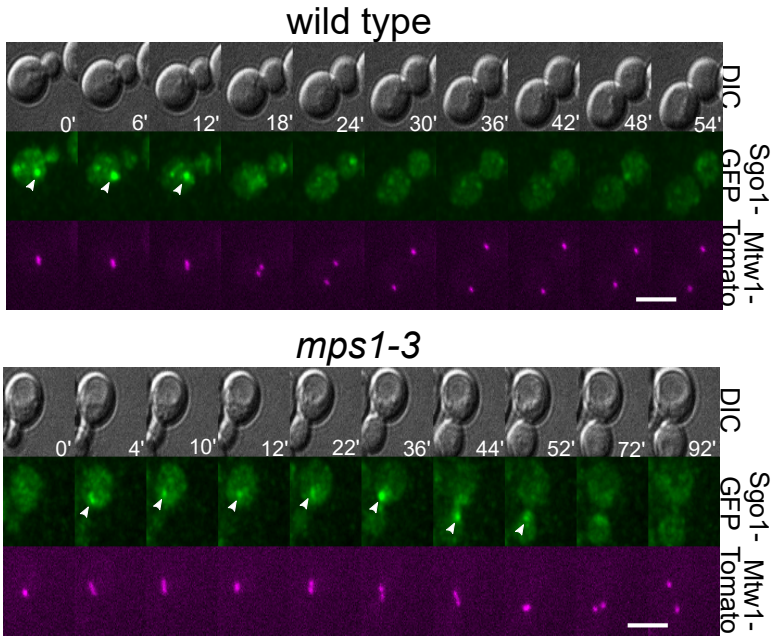

B

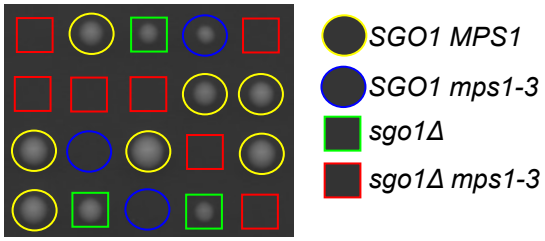

	Sgo1 localization		n
	yes	no	
wild type	100%	/	21
mps1-3	43%	57%	65

C

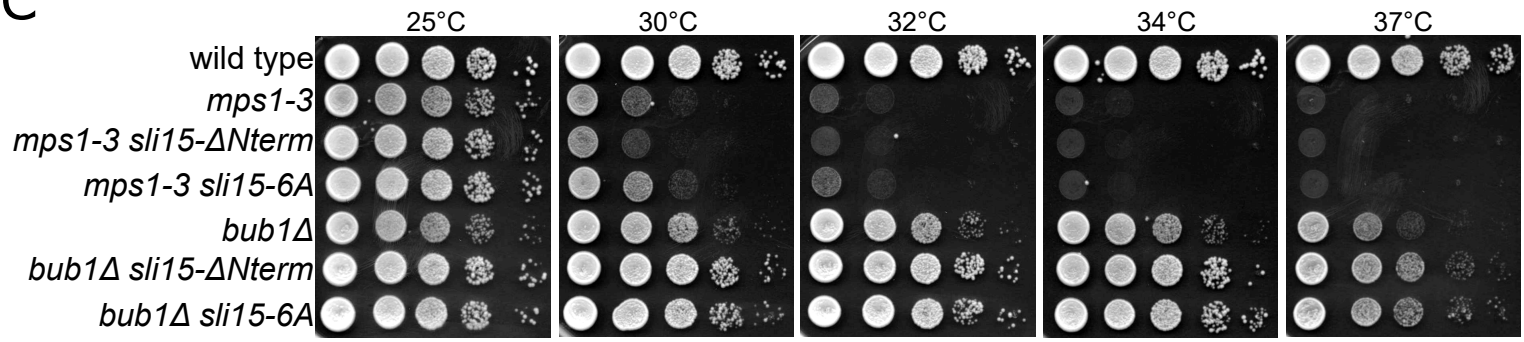

D

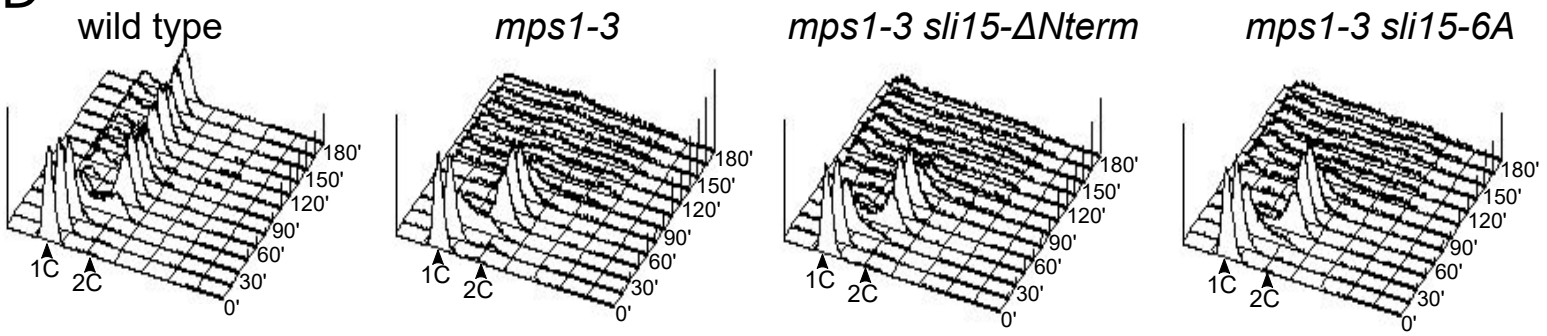

E